

TECHNICAL REPORT 04-09

A Report of the Spent Fuel Stability (SFS) Project
of the 5th Euratom Framework Program

**Spent Fuel Evolution under
Disposal Conditions**

**Synthesis of Results from the EU
Spent Fuel Stability (SFS) Project**

March 2005

TECHNICAL REPORT 04-09

A Report of the Spent Fuel Stability (SFS) Project
of the 5th Euratom Framework Program

**Spent Fuel Evolution under
Disposal Conditions**

**Synthesis of Results from the EU
Spent Fuel Stability (SFS) Project**

March 2005

This report was prepared by:

L.H. Johnson (ed.)	Nagra, Wettingen, Switzerland
C. Poinssot	CEA, Saclay
C. Ferry	
P. Lovera	
A. Poulesquen	
F. Miserque	
C. Corbel	
J.M. Cavedon	PSI
Z. Andriambololona	ANDRA
D. Wegen	ITU, Karlsruhe
P. Carbol	
J.P. Glatz	
J. Cobos-Sabate	
D. Serrano	
V. Rondinella	
T. Wiss	
B. Grambow	SUBATECH, école de Mines, Nantes
K. Spahiu	SKB, Stockholm
M. Kelm	Forschungszentrum, Karlsruhe
V. Metz	
A. Loida	
B. Kienzler	
T. Lundström	Studsvik, Sweden
H. Christensen	
M. Jonsson	
J. de Pablo	UPC, Barcelona
M. Rovira	
F. Clarens	
I. Casas	
A. Martinez-Esparza	ENRESA, Madrid
J. Gago	
J. Bruno	Enviros, Barcelona
E. Cera	
J. Merino	
A. Gonzalez de la Huebra	CIEMAT, Madrid
E. Iglesias	
J. Quinones	
C. Cachoir	SCK·CEN, Brussels
K. Lemmens	
G. Mayer	Colenco, Baden, Switzerland
C. Jegou	CEA, Marcoule

Abstract

Over the period 2002-2004, a large number of European organisations cooperated on the EU Project SFS – Spent Fuel Stability under disposal conditions. The objective of the SFS Project was to develop a reliable and robust model for the spent fuel source term which can be used in performance assessment exercises by the waste management agencies responsible for assessing the feasibility and safety of potential geological disposal systems for spent fuel, whatever the countries and disposal system designs may be.

A new model for short-term release of fission products (Instant Release Fraction or IRF) was developed based on the anticipated fission product release from various fuel microstructures (gap, rim, grain boundaries) and the potential solid-state diffusion of fission products prior to canister breaching. For the oxide matrix of the spent fuel, a Matrix Alteration Model (MAM) was developed, which is linked to the production of oxidants by water radiolysis at the fuel interface, the oxidation of the fuel interface by radiolytic oxidants and the subsequent release of uranium under the influence of aqueous ligands. A large set of experimental data was therefore acquired in order to (i) upgrade the current radiolytic kinetic scheme, (ii) determine the relationship between fuel alteration rate and alpha activity by performing experiments on alpha-doped samples of UO_2 and (iii) experimentally test the potential inhibition effect of hydrogen on fuel dissolution. Based on these results, a new MAM was developed that was calibrated using experiments on inactive UO_2 samples, although the hydrogen effects remain to be incorporated completely into the model. The integrated model combining the IRF and MAM was used to illustrate long-term performance of representative spent fuel disposed of in granite, salt and clay host rock environments.

The findings of the SFS Project have significantly enhanced the understanding of phenomena that may affect radionuclide release from spent fuel under disposal conditions and have helped to more clearly identify areas in which uncertainties should be reduced through future research.

Zusammenfassung

Während des Zeitraums 2002-2004 fand das EU-Projekt SFS – Spent Fuel Stability under disposal conditions (Brennstoffstabilität unter Lagerbedingungen) unter Mitbeteiligung vieler europäischer Organisationen statt. Die Zielsetzung des SFS-Projekts war die Entwicklung eines verlässlichen und robusten Modells für den Brennstoff-Quellterm, der für Sicherheitsanalysen von geologischen Lagern von abgebrannten Brennelementen eingesetzt werden kann. Dabei sollte dieser Quellterm unabhängig vom länderspezifischen Lagerungssystem verwendet werden können.

Es wurde ein neues Modell für die kurzzeitige Freisetzung der Spaltprodukte (Instant Release Fraction oder IRF) entwickelt, das auf der erwarteten Spaltproduktfreisetzung von verschiedenen Brennstoff-Mikrostrukturen (Spalt, Randbereich, Korngrenzen) und auf der potentiellen Festphasendiffusion von Spaltprodukten vor dem Behälterversagen beruht. Für der Oxidmatrix des Brennstoffs wurde ein Matrixumwandlungsmodell (Matrix Alteration Model – MAM) entwickelt, das mit der Bildung von Oxidationsmitteln durch die Wasserradiolyse an der Brennstoffoberfläche, der Oxidation der Brennstoffoberfläche durch radiolytische Oxidationsmittel und der nachfolgenden Uranfreisetzung unter dem Einfluss von wässrigen Liganden verknüpft ist. Dieses Modell erforderte einen grossen experimentellen Datensatz, (i) um das gängige radiolytische kinetische Modell zu ergänzen, (ii) um die Wechselwirkung zwischen der Brennstoff-Auflösungsrate und der Alpha-Aktivität durch Experimente an alpha-dotierten UO_2 -Proben zu bestimmen, und (iii) um den potentiellen Inhibitionseffekt durch Wasserstoff auf die Brennstoffauflösung zu testen. Gestützt auf diese Resultate wurde ein neues MAM-Modell entwickelt, das mit Hilfe von Experimenten mit inaktiven UO_2 -Proben geeicht wurde, obwohl die Berücksichtigung der Wasserstoffeffekte noch aussteht. Das integrierte Modell, welches die IRF und das MAM kombiniert, wurde für repräsentative Lager von abgebrannten Brennelementen in Granit-, Salz- und Tongestein-Umgebungen angewendet.

Die Erkenntnisse aus dem SFS-Projekt haben entscheidend zum Verständnis der Phänomene beigetragen, welche die Radionuklidfreisetzung aus den abgebrannten Brennelementen unter Lagerbedingungen beeinflussen. Ausserdem hat das SFS-Projekt dazu beigetragen, zukünftige Forschungsarbeiten zu fokussieren und damit gezielt Unsicherheiten zu reduzieren.

Résumé

Entre 2002 et 2004, de nombreuses organisations européennes ont coopéré au projet SFS (Spent Fuel Stability) de la CE, concernant la stabilité des assemblages de combustibles usés en condition de stockage. L'objectif du projet SFS était de développer un modèle fiable et robuste décrivant le terme source des assemblages de combustibles usés. Le modèle a été élaboré en particulier pour être utilisé par les agences de gestion des déchets chargées d'évaluer la faisabilité et la sûreté de systèmes potentiels de stockage géologique pour assemblages de combustibles usés; il peut être appliqué dans le cadre d'analyse de sûreté quels que soient le pays et l'architecture de dépôt.

Un nouveau modèle a été mis au point pour décrire le relâchement des produits de fission à court terme (Instant Release Fraction, IRF). Il repose sur un pronostic des produits de fission relâchés par diverses microstructures du combustible (vides, arêtes, bordures de grains) et d'une diffusion potentielle des produits de fission à travers le solide (solide state diffusion) avant la rupture du conteneur. Quant à la matrice d'oxyde du combustible usé, elle est décrite par le Modèle d'Altération de la Matrice (MAM); celui-ci prend en compte la production d'oxydants par radiolyse de l'eau à l'interface avec le combustible, l'oxydation de la surface du combustible par les oxydants produits par radiolyse, ainsi que le relâchement subséquent d'uranium sous l'influence des ligands aqueux. En conséquence, un ensemble important de données expérimentales fut recueilli dans le but (i) d'améliorer l'actuel schéma des cinétiques de radiolyse, (ii) de déterminer la relation entre le taux d'altération du combustible et l'activité alpha en menant des expérimentations sur des échantillons d' UO_2 dopés aux rayons alpha, et (iii) de tester expérimentalement un possible effet inhibiteur de l'hydrogène sur la dissolution du combustible. Ces résultats ont permis de développer un nouveau MAM et de l'étalonner sur la base d'expérimentations conduites sur des échantillons d' UO_2 inactifs; il reste cependant à y incorporer entièrement l'effet de l'hydrogène. Un modèle intégrant IRF et MAM a finalement servi à illustrer le comportement à long terme d'assemblages représentatifs de combustibles usés stockés dans des roches d'accueil granitique, saline et argileuse.

Les conclusions du projet SFS ont amélioré de façon significative la compréhension des phénomènes qui peuvent affecter le relâchement des radionucléides des assemblages de combustibles usés dans des conditions de stockage; elles permettent, par ailleurs, d'identifier plus précisément les domaines dans lesquelles il reste des incertitudes et où de futures recherches seraient nécessaires.

List of Contents

Abstract	I
Zusammenfassung.....	II
Résumé	III
List of Contents	V
List of Tables.....	VII
List of Figures	VII
1 Introduction	1
1.1 SFS Project Objectives	1
1.2 Scope and Objectives of the Present Report.....	1
2 Fuel Types and their Characteristics	3
3 Repository Conditions for SF Evolution.....	5
3.1 Reference EBS Concepts.....	5
3.2 Boundary Conditions and Chemistry.....	5
3.3 Mass transport conditions.....	8
4 The IRF Model.....	9
4.1 Overview	9
4.2 Fission gas release	9
4.3 Leaching of fission products and IRF estimates	10
4.4 Closed System Evolution.....	11
5 Experimental and Modelling Studies of Radiolysis and Effects of H₂	15
5.1 Radiolytic Modelling and Model Evaluation.....	15
5.2 Experimental Studies of UO ₂ and SF Dissolution	15
6 The Matrix Alteration Model (MAM)	19
6.1 Overview	19
6.2 Validation of the MAM	19
6.3 Time-dependent Calculations Using the MAM for the Granite and Clay Cases	20
6.4 Application of MAM to Salt Repository Conditions.....	22
6.5 Overview of the Integrated Model for Spent Fuel Dissolution.....	23
7 Spent Fuel Evolution Over Time: Performance Assessment Perspectives	27
7.1 Introduction	27
7.2 Comparison of alteration rates calculated using the MAM with experimentally-derived rates for H ₂ -dominated systems	27
7.3 Influence of Burnup and Container Breaching Time on SF Dissolution Rates Calculated with the MAM	28

7.4	Relative contributions of IRF, Alpha-enhanced Diffusion and Matrix Dissolution to Radionuclide Release	30
7.5	Results of calculations using the integrated model for radionuclide release from spent fuel	32
8	Summary	37
9	References.....	39
App. 1:	Mass transport conditions at the interface between the near field and the host rock	41

List of Tables

Tab. 1-1:	Main issues, prior status of research and outcomes of the SFS Project	2
Tab. 3-1:	Chemical and transport conditions for a breached spent fuel container in a granite or clay repository	7
Tab. 3-2:	Chemical and transport conditions for a breached spent fuel container in salt repository	8
Tab. 4-1:	Gap and GB inventory estimates (% of total inventory) for various radionuclides for PWR fuel, based on best estimate values for burnups of 48 GWd/t _{IHM} or less and pessimistic estimate values for higher burnups.	11
Tab. 4-2:	Gap and GB inventory estimates (% of total inventory) for various radionuclides for BWR fuel	11
Tab. 6-1:	Comparison of spent fuel dissolution rates at 1 000 years for granite, clay and salt porewaters	22
Tab. 6-2:	Parameter values relevant to mass transport at the interface between the near field and the host rock	25
Tab. 6-3:	Fuel and container parameters	25

List of Figures

Fig. 4-1:	Fractional Cs release (gap plus grain boundaries compared to FGR for UO ₂ fuels (Johnson et al. 2004)	10
Fig. 4-2:	Comparison of α self-irradiation enhanced diffusion coefficients calculated with several alternative models (based on Lovera et al. 2003, with addition of values from Olander 2004)	12
Fig. 4-3:	Calculated released fraction from grains due to α self-irradiation enhanced diffusion for UO ₂ fuels with burnups of 45, 55, 65 and 75 GWd/t _{IHM} (Lovera et al. 2003)	13
Fig. 5-1:	Alpha-activity of various spent fuels as compared to the alpha activity of doped UO ₂ samples used in the SFS Project	16
Fig. 5-2:	Effects of alpha radiolysis on U dissolution under anoxic conditions: comparison of results from samples with no alpha-doping (UO ₂ -0), 1 % ²³³ U (UO ₂ -U ₁) and 10 % ²³³ U (UO ₂ -U ₁₀). Details are reported in Cachoir et al.	17
Fig. 5-3:	Measured total U and H ₂ concentrations in solution in contact with UO ₂ doped with 10 % ²³³ U (details are discussed in Carbol et al.	18
Fig. 6-1:	UO ₂ dissolution rate calculated using the MAM model compared to results from flow-through experiments with unirradiated UO ₂ at various pH values with [H ₂ O ₂] = 1 × 10 ⁻⁵ M. See Merino et al. (in press) for details.	20
Fig. 6-2:	Evolution of the molecular species concentrations in solution in granite reference case	21
Fig. 6-3:	Time-dependent alteration rate calculated with the MAM for spent fuel (burnup = 41 GWd/t _{IHM}) in granite and clay porewaters	21

Fig. 6-4:	Fraction of reference spent fuel (burnup = 41 GWd/t _{IHM}) altered as a function of time in the three reference groundwater (granite, clay, salt brine), calculated using the MAM.....	23
Fig. 6-5:	Illustration of the conceptual model used in the Integrated SFS Model.....	23
Fig. 7-1:	Comparison of fractional dissolution rates calculated using the MAM with the range of values estimated from experimental studies of dissolution of alpha-doped UO ₂ and spent fuel in the presence of H ₂	28
Fig. 7-2:	Effect of fuel burnup on fuel alteration rate as calculated with the MAM.....	29
Fig. 7-3:	Effect of burnup on fraction of fuel altered over time for granite groundwater.....	29
Fig. 7-4:	Effect of canister breaching time on the time-dependent alteration rate as calculated with the MAM (granite case), for a fuel burnup of 41 GWd/t _{IHM} . Only the IRF at t = 0 is shown here.....	30
Fig. 7-5:	Integrated release of I-129 from spent fuel with a burnup of 41 GWd/t _{IHM} (granite case) considering matrix dissolution only (lower curve), matrix dissolution plus IRF (t = 0) and matrix dissolution plus IRF (t = 0) plus IRF (t).....	31
Fig. 7-6:	Integrated release of I-129 from spent PWR fuel with a burnup of 60 GWd/t _{IHM} (granite case), considering matrix dissolution only (lower curve), matrix dissolution plus IRF (t = 0) and matrix dissolution plus IRF (t = 0) plus IRF (t).....	31
Fig. 7-7:	The distribution of I-129 as a function of time, showing the amounts in the fuel matrix, IRF and released from the container, for fuel with a burnup of 41 GWd/t _{IHM}	32
Fig. 7-8:	The distribution of Pu-239 as a function of time, showing the amounts in the fuel matrix, precipitate within the container (solubility = 7 × 10 ⁻⁹ mol/l) and released from the container, for a fuel burnup of 60 GWd/t _{IHM} (granite case).....	33
Fig. 7-9:	The distribution of I-129 as a function of time for the case of containers of spent fuel (burnup = 41 GWd/t _{IHM}) having breaching times of 1 000 years in repositories in granite, clay and salt.....	34
Fig. 7-10:	The distribution of Np-237 as a function of time for the case of containers of spent fuel (burnup = 41 GWd/t _{IHM}) having a breaching time of 1 000 years in repositories in granite, clay and salt.....	35

1 Introduction

1.1 SFS Project Objectives

The fundamental objective of the SFS Project is to develop a reliable and robust model for the spent fuel source term which can be used with confidence in performance assessment exercises by the waste management agencies responsible for assessing the feasibility and safety of a potential geological disposal system, whatever the countries and disposal system designs are.

The RN source term for spent nuclear fuel is considered to comprise two contributions:

- (i) The so-called Instant Release Fraction (IRF), which corresponds to the radionuclides located at the interface between the cladding and the pellet and in the grain boundaries, which is expected to be rapidly released when the container is breached and water ingress occurs and
- (ii) The radionuclides which are located within the grains and which are released with the alteration of the grains. This contribution is often referred to as the matrix contribution. Two mechanisms have been invoked as the potential long-term governing mechanisms:
 - a dissolution controlled by the solubility of grains (roughly the UO_2 solubility) and the mass transport conditions, or
 - oxidative dissolution related to the existence of a significant but decreasing α activity at the fuel/water interface which yields oxidative species by water radiolysis, which then may react with the fuel (radiolytic mechanism).

The SFS Project has further developed these aspects by evaluating literature data, performing radiolysis and spent fuel dissolution experiments and developing models. The outcome is a new IRF model, a Matrix Alteration Model (MAM) and a large body of new experimental and modeling data relevant to spent fuel dissolution in a geological repository.

Fundamental achievements of the project, in the context of the state-of-the-art at the beginning of the SFS Project are outlined in Table 1-1.

1.2 Scope and Objectives of the Present Report

The various SFS Project reports provide detailed discussion of modeling and experimental studies performed throughout the duration of the Project. The outcomes of these studies are summarized and brought together here through the development of an integrated dissolution model for spent fuel and a discussion of the overall findings of the project in a performance assessment context. This provides a method of illustrating the relative significance of the various radionuclide release processes and of the uncertainties in the rates. Results from the integrated model, which are presented in Section 7, illustrate aspects of the IRF model (Section 4) and the MAM (Section 6) and are presented along with a discussion of important supporting evidence (summarized in Section 5). Uncertainties and reliability of data and model results, including the limitations of the model with respect to spent fuel variability (e.g. the range of applicability in relation to burnup and composition (UO_2 , MOX)) and geological medium are discussed.

Tab. 1-1: Main issues, prior status of research and outcomes of the SFS Project

Issue	Status Prior to SFS Project	Outcomes of the SFS Project
Source term predictions for spent fuel as confinement matrix	<ul style="list-style-type: none"> • Current best estimates predict fast release of labile bound radionuclides and slow release (with a wide uncertainty band) from the fuel matrix under the expected low Eh conditions • Some models available, but uncertainty in predictions is high. 	A matrix alteration model (MAM) relevant to reducing repository conditions and incorporating radiolytic effects was developed. Uncertainties have been reduced in dissolution rates.
Quantification of instant release fraction (IRF)	<ul style="list-style-type: none"> • Rough estimates of the IRF for fresh fuels (< 15 yr old) are known (although representativeness of data is uncertain). The data is only partially representative of fuel which will be in contact with water in a real repository. • Pessimistic assumptions on relevant nuclide inventories result in high radiological risk contribution • IRF values vary by more than a factor of 10. 	<p>Available literature data on the IRF was reviewed and analysed and solid-state diffusion models were developed for RN in UO₂, permitting transport to grain boundaries before water access to be modelled.</p> <p>A larger range of fuel burnups have been evaluated. Pessimistic assumptions remain in various aspects of the IRF model, in particular for MOX fuel.</p>
Fuel Matrix stability under irradiation	<ul style="list-style-type: none"> • Spent fuel matrix is very stable in the absence of oxidants and the only long term source for oxidants is alpha radiolysis of water. • Radiolysis models incorporate large uncertainties and are not able to relate the decreasing residual activity to a spent fuel alteration rate • Activity levels of fresh fuels (those with a high γ field) are not representative of old ones. • Hydrogen resulting from container corrosion may compete with radiolytic oxygen generation and slows down spent fuel corrosion rates although no model is available. 	<p>A broad range of experimental and radiolytic modelling studies have clarified the reactions relevant to dissolution.</p> <p>Corrosion rates of UO₂ have been measured using doped UO₂ with activity levels representative of different fuel ages, including under hydrogen pressure conditions relevant to a repository. In the absence of hydrogen, a threshold alpha-activity was identified, below which rates are the same as for UO₂. With hydrogen present, dissolution rates are markedly lower. This is also true for spent fuel dissolution experiments.</p>

2 Fuel Types and their Characteristics

The reactor fuels in wide use in Europe include:

- PWR UO₂ fuel, with typical burnups of 35 - 55 GWd/t_{IHM} (tons initial heavy metal) and maximum burnups of ~ 75 GWd/t_{IHM}
- BWR UO₂ fuel, with typical burnups of 35 - 50 GWd/t_{IHM} and maximum burnups of ~ 60 GWd/t_{IHM}
- PWR and BWR MOX fuel, with typical burnups of 35 - 50 GWd/t_{IHM} and maximum burnups of ~ 60 GWd/t_{IHM}

The performance of these fuel types in a repository has been considered in the SFS Project. Most of the dissolution data available are for spent UO₂ fuel with burnups up to 50 GWd/t_{IHM}, although assessments of the IRF performed in the SFS Project have been made for high burnup UO₂ fuel and for MOX fuel. Radionuclide release from Zircaloy is not evaluated here, although the expected corrosion of Zircaloy under repository conditions has been reviewed and is summarised in Johnson et al. (2004).

3 Repository Conditions for SF Evolution

3.1 Reference EBS Concepts

Two reference EBS types are considered in the SFS Project. These are:

1. an EBS for a granite or clay host rock, consisting of a container for spent fuel surrounded by a clay (bentonite) buffer. The container may be carbon steel, stainless steel or a copper shell with a cast iron insert.
2. an EBS for salt host rock, consisting of a steel container surrounded by salt backfill.

Inside the container there will be a number of PWR or BWR fuel assemblies, which may comprise UO_2 or MOX fuel and associated Zircaloy and steel fuel assembly hardware, and backfilling materials (inert filler such as silica sand or a metallic insert, or simply helium or air). For calculations of release of radionuclides from a hypothetical container of SF in a repository, presented in Section 7, containers are assumed to have an internal void volume of 0.5 m^3 (calculations show that the releases are insensitive to the size of the void volume).

3.2 Boundary Conditions and Chemistry

Details of the chemical and mass transport conditions in granite, clay and salt host rocks are given in Andriambolona and Johnson (2003). Two important time domains can be distinguished, which have a bearing on the evolution of the fuel:

1. before the water comes into contact with the assembly inside the container ($T > 100 \text{ }^\circ\text{C}$). Changes may occur to the properties of the Zircaloy (not addressed in SFS Project) and the fuel matrix due to solid-state processes, which may influence subsequent radionuclide release. These aspects of Closed System Evolution are discussed in Section 4 under the IRF Model.
2. after container breaching (container design lifetime of $\sim 1\,000$ years is assumed in the SFS Project for model calculations, although lifetimes are expected to be at least $10\,000$ years for a steel container (Johnson & King 2003) to $> 100\,000$ years for a copper container (SKB 1999)), when corrosion of cladding and dissolution of the spent fuel might begin. Temperatures within a breached container into which water has flowed are expected to initially be in the range of 25 to $60 \text{ }^\circ\text{C}$, depending on ambient host rock temperature (the latter ranges from $\sim 15 \text{ }^\circ\text{C}$ to $\sim 40 \text{ }^\circ\text{C}$ and is a function of repository depth, location and rock type). In the long term ($> 10\,000$ years), temperatures within the breached saturated container will reach ambient values. The early container breaching scenario (i.e. container defect scenario) is not addressed explicitly in the SFS Project. Nonetheless, given the expectation of slow transport of water through a defect, the conditions of exposure of spent fuel to water may be similar to those outlined above.

The conditions to which spent fuel is exposed upon container breaching depend on the nature of the repository host rock, the backfill materials, the container material(s) and the interaction of groundwater with all these components. Furthermore, transport conditions can influence these interactions. Finally, chemical changes induced by the radiation emitted by the fuel may be significant once the container is breached and water ingress occurs.

Mass transport conditions both outside the container prior to breaching and inside a breached container can be considered diffusion-controlled for all these systems, even though flow rates in the surrounding rock may vary considerably, because diffusion in the backfill (bentonite or salt)

controls mass transport rates, except under disruptive scenario conditions. As discussed below, there is considerable overlap in the ranges of chemical parameters for clay and granite host rocks, thus an argument can be made that they constitute a single family of groundwaters with parameter variation ranges for the pH, Eh and concentrations of important species, with a relatively broad range of salinities possible (up to sea water TDS). Repository host rock types considered here include:

Clay host rock

- claystones such as Opalinus Clay or Callovo-Oxfordian Clay, characterised by low porosity, slightly saline, strongly reducing porewaters and extremely low hydraulic conductivity ($\sim 10^{-14} \text{ m s}^{-1}$)
- Boom Clay, higher porosity, low permeability ($\sim 10^{-12} \text{ m s}^{-1}$), but having very low porewater salinity ($\sim 0.01 \text{ mo/l TDS}$).

Granite Host Rock

- crystalline rocks of the Fenno-Scandian Shield are characterised by fracture flow with a broad range of hydraulic conductivities and water chemistries that are typically low salinity (although future evolution scenarios consider higher salinities).

Salt Host Rock

- If water is present, saturated brine chemistry is expected.

Note that pore water chemistries in clay and granite repositories will be conditioned by the bentonite buffer surrounding the container, by container corrosion and by radiolysis of water. Representative water chemistries and hydraulic conditions, to which the SF will be exposed after container breaching, are briefly summarised in Tables 3-1 and 3-2. The experimental studies performed within the SFS project cover the full range of these conditions.

Tab. 3-1: Chemical and transport conditions for a breached spent fuel container in a granite or clay repository

Parameter	Name	Variation range
Temperature		
	T	25 °C - 60 °C
Hydraulic parameters in bentonite		
Diffusion coefficient (species dependent)	D_e	$3 \times 10^{-12} \text{ m}^2/\text{s}$ (anions) $2 \times 10^{-10} \text{ m}^2/\text{s}$ (cations)
Porosity	ϵ	0.36
Hydraulic conductivity	k	$< 10^{-12} \text{ m s}^{-1}$
Composition of the ground water		
	pH	7 - 10
	Eh (mV)	-130 (pH 7) to - 300 (pH 8)
Carbonate system (mol/l)	HCO_3^-	$10^{-4} - 6 \times 10^{-2}$
Major cations (mol/l)	Na^+	$2 \times 10^{-3} - 0.4$
	K^+	$10^{-4} - 10^{-3}$
	Ca^{++}	$10^{-4} - 10^{-2}$
	Mg^{++}	$10^{-5} - 2 \times 10^{-3}$
Species influencing redox conditions	PH_2	1 to 10 MPa
	Fe(II)	$1 \times 10^{-7} - 3 \times 10^{-4}$
	Fe(II)/Fe(III) phases	magnetite, siderite, green rust
Major Anions (mol/l)	Cl^-	$1 \times 10^{-3} - 0.4$ (min. - Boom Clay, max. - saline water in granite)
	SO_4^{--}	$10^{-5} - 0.14$

Tab. 3-2: Chemical and transport conditions for a breached spent fuel container in salt repository

Parameter	Name	Variation range
Temperature	T (°C)	25 - 100
Hydraulic parameters		
Diffusion coefficient		
Porosity		
Composition of the ground water		
	pH	7 - 9
	Eh	
Total Carbonate (mol/l)	HCO ³⁻	
Major cations (mol/l)	Na ⁺	~ 6
	K ⁺	> 1
	Ca ⁺⁺	> 0.2
	Mg ⁺⁺	> 5
Anions (mol/l)	SO ₄ ⁻⁻	> 2
	Cl ⁻	~ 6
Species controlling redox conditions	Fe(II)/Fe(III)	magnetite, green rust
	pH ₂	10 - 20 MPa

3.3 Mass transport conditions

Except under disruptive scenario conditions, transport in the vicinity of a spent fuel container will be diffusive. The hydrogen concentration in solution in the container after breaching will depend on the anaerobic corrosion rate of the container material in question and the diffusive transport rate of hydrogen across the buffer into the surrounding rock. Calculations of the production of H₂ and its transport from the container have been performed for granite, clay and salt repository conditions. In most cases, H₂ partial pressures are expected to be 5 to 10 MPa because gas production rates exceed the diffusive transport capacity of the bentonite. In the case of the Boom Clay repository, the H₂ pressure may be somewhat lower, perhaps 1 MPa, because of the use of a stainless steel container with a lower corrosion rate. Assuming a carbon steel corrosion rate of ~ 1 µm/a, high hydrogen partial pressures are likely to be sustained for very long periods (up to ~ 100 000 years). Note that calculations using the MAM have used a conservative value for initial hydrogen pressure of 0.3 MPa and this value is assumed to be sustained for all model calculation times (see Section 6).

The basic elements of the evolution of the system as described above and summarised in Tables 3-1 and 3-2 have been taken into consideration in the experimental program in the SFS Project and in the model development and calculations.

4 The IRF Model

4.1 Overview

The short-term release of radionuclides that occurs when spent fuel comes into contact with water is called the IRF (instant release fraction). It comprises rapid release of segregated radionuclides from the gap and fractures and slower release (though still rapid compared to matrix dissolution) from grain boundaries and pores. The degree of segregation of the various radionuclides is highly dependent on in-reactor fuel operating parameters such as linear power rating and burnup. Furthermore, after discharge from the reactor, solid-state alpha-radiation enhanced diffusion of radionuclides to grain boundaries may occur prior to disposal container breaching. All these aspects have been assessed quantitatively in the SFS Project in Johnson et al. (2004) and Lovera et al. (2004), focusing on the following elements:

- evaluation of fission gas release (FGR) as a function of burnup based on published and new data for PWR and BWR UO₂ and MOX fuel,
- review of leaching studies for various fuels (UO₂ and MOX) and correlation of leaching data with FGR data,
- assessment of the importance of fission product segregation due to the rim effect at burnups above 40 GWd/t and its possible contribution to the IRF and
- assessment of the importance of solid-state diffusion phenomena in spent fuel in the context of the IRF, through application of various models for diffusion enhanced by alpha-radiation, which could lead to gradual accumulation of some fission products at grain boundaries and thus add a time-dependent component to the IRF.

4.2 Fission gas release

The release of fission gas from UO₂ fuel is strongly correlated with the linear heat rating, which is dependent on fuel temperature. Optimization of fuel assembly designs and irradiation conditions help to ensure that linear heat ratings are kept low and thus FGR is minimized. As a result, FGR values are typically < 1 % at burnups below 40 GWd/t_{IHM}, for PWR fuel and < 3 % for BWR fuel. At higher burnups, a reduction of thermal conductivity increases the fuel temperatures, thus FGR tends to increase, reaching typical values of 3 % at 50 GWd/t_{IHM} and 6 % at 70 GWd/t_{IHM} for PWR fuel.

In higher burnup UO₂ fuel (> 40 GWd/t_{IHM}), a restructured region appears around the periphery of the UO₂ pellet due to the high local burnup. This rim region is characterized by small grains (around 0.5 µm) and large closed porosity (10 to 15 %), with over-pressured fission gas bubbles of micrometre size.

Based on a comprehensive review by Koo et al. (2003), it has been possible to estimate the fraction of the inventory of fission gas in the rim region and, assuming similar behaviour, the quantity of radionuclides such as I-129. The rim thickness increases from about 50 µm at a burnup of 50 GWd/t_{IHM} to 120 µm and 170 µm at 65 and 75 GWd/t_{IHM}. In spite of the high degree of restructuring of the rim, fission gas is retained in the new rim pore structure, which explains the low overall fission gas release for PWR fuels at high burnup. Nonetheless, the fission gas in this region can be considered released from the fuel matrix, even though it is not released to the void space in the fuel rod. Similarly, other fission products that are not in solid solution in UO₂ can be expected to be released from the grains during restructuring. As a result, from the perspective of release under disposal conditions, such fission products can be con-

sidered to belong to the grain boundary inventory of the fuel and be potentially available for release if groundwater penetrates grain boundaries.

For MOX fuel, FGR is considerably higher, reaching typical values of 5 % at 40 - 50 GWd/t_{IHM}. In addition, Pu-rich agglomerates in MOX fuel are highly porous and up to 50 % of the fission gas may be present in the pores in such grains. The significance of this is not clear, as little leaching data is available for such fuels.

4.3 Leaching of fission products and IRF estimates

The data on leaching of fission products from the gap and grain boundaries has been comprehensively reviewed and correlated with FGR data (Johnson et al. 2004). An illustration of one of these correlations is shown in Figure 4-1, which shows the IRF (gap plus grain boundary release) for ¹³⁷Cs compared to FGR. Combined with the estimates of FG segregated within the rim region, the approach provides a basis for estimating the IRF for PWR and BWR fuel over a burnup range from 37 to 75 GWd/t_{IHM}. These estimates are given in Tables 4-1 and 4-2. They are based on the assumption that all of the indicated fission products are available for immediate release upon exposure to water because they are present in the gap or at grain boundaries throughout the fuel, including within pores in the rim region. Note that the large increase in the IRF above 48 GWd/t_{IHM} is principally due to release within the rim region. In one important respect, these estimates may be considered rather pessimistic because they assume instant access of water to all closed pores. Nonetheless, from another perspective, important uncertainties remain unresolved regarding long-term stability of grain boundaries where such pores exist, in particular due to build-up of He gas pressure over time, which may lead to microcracking and eventual exposure of closed pores to groundwater.

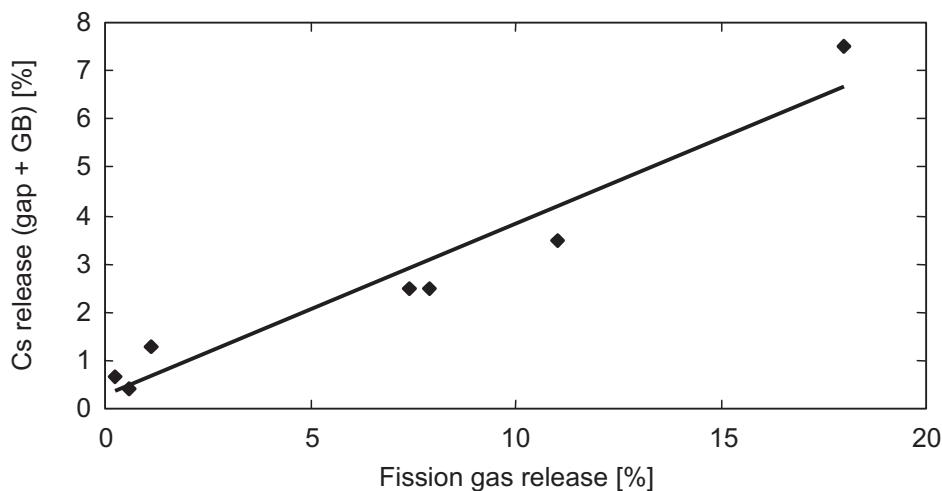


Fig. 4-1: Fractional Cs release (gap plus grain boundaries compared to FGR for UO₂ fuels (Johnson et al. 2004)

The data on IRF of MOX fuels remain extremely limited and more studies are required to make reliable estimates. At present, one can only acknowledge the potential for IRF values of up to 50 %, although no experimental confirmation of such values exists.

Tab. 4-1: Gap and GB inventory estimates (% of total inventory) for various radionuclides for PWR fuel, based on best estimate values for burnups of 48 GWd/t_{IHM} or less and pessimistic estimate values for higher burnups.

BURNUP	37		41		48		60		75	
RN	Gap	GB								
fission gas	1	1	1	1	1	3	4	8	8	14
¹⁴ C*	10		10		10		10		10	
³⁶ Cl	5		5		10		12		25	
⁷⁹ Se	0.1	1	0.1	1	0.1	2	0.4	8	0.8	14
⁹⁰ Sr	1	-	1	-	1	-	1	8	1	14
⁹⁹ Tc	0	1	0	1	0	2	0	8	0	14
¹⁰⁷ Pd	0	1	0	1	0	2	0	8	0	14
¹²⁶ Sn	0.01	1	0.01	1	0.01	2	0.01	8	0.01	14
¹²⁹ I	1	2	1	2	1	3	4	8	8	14
¹³⁵ Cs	1	1	1	1	1.5	1	4	8	8	14
¹³⁷ Cs	1	1	1	1	1.5	1	4	8	8	14

Tab. 4-2: Gap and GB inventory estimates (% of total inventory) for various radionuclides for BWR fuel

BURNUP	37		41		48	
RN	Gap	GB	Gap	GB	Gap	GB
fission gas	1	1	1	1	5	3
¹⁴ C*	10	10	10	10	10	10
³⁶ Cl	5		5		13	
⁷⁹ Se	0.1	1	0.1	1	0.5	2
⁹⁰ Sr	1	1	1	1	1	1
⁹⁹ Tc	0	1	0	1	0	2
¹⁰⁷ Pd	0	1	0	1	0	2
¹²⁶ Sn	0.01	1	0.01	1	0.01	2
¹²⁹ I	1	2	1	2	5	4
¹³⁵ Cs	1	1	1	1	2	3
¹³⁷ Cs	1	1	1	1	2	3

4.4 Closed System Evolution

Some solid-state processes have been identified in the SFS Project that may give rise to changes in fuel properties while the container is unbreached. As noted above, He pressure will build up in closed pores as a result of accumulation from actinide decay and diffusion through the fuel grains. The studies performed by the CEA in association with the SFS Project are unable as yet to clarify the diffusion coefficients and effects of pressure buildup, thus this issue remains unresolved and should be explored in future studies.

Another process of potential significance is diffusion of fission products to grain boundaries caused by effects from α -decay. Some theoretical approaches have been developed in order to evaluate the diffusion coefficient resulting from α self-irradiation. They are based on calculations of ballistic displacements of atoms which may be enhanced by the migration of defects created by cascades due to the recoil atom. Results are reported and discussed by Lovera et al. (2003). The self-irradiation enhanced diffusion coefficient is expected to decrease with time proportionally with the volume α - activity in the spent fuel.

The α -enhanced diffusion process in the grains would increase the quantities of radionuclides present in the labile zone (pores and grain boundaries) of the rod at container failure. This mechanism has not yet been experimentally studied and verified. Results obtained with various alternative models are shown in Figure 4-2. The results cover several orders of magnitude and no experimental data are yet available to discriminate between these alternative estimates. In the SFS Project, values at the higher end (extrapolation from in-reactor data, Figure 4-2) have been used for estimating the contribution of α self-irradiation enhanced diffusion to the IRF. The effect on the IRF, i.e. the time-dependent IRF, is shown in Figure 4-3 for several burnup values.

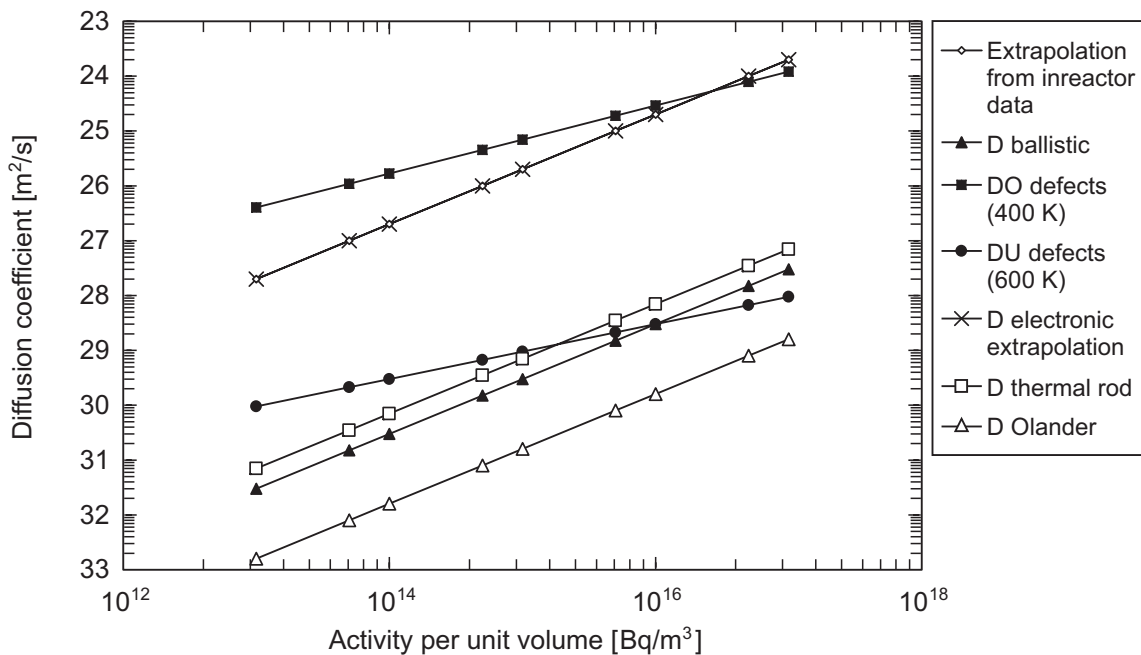


Fig. 4-2: Comparison of α self-irradiation enhanced diffusion coefficients calculated with several alternative models (based on Lovera et al. 2003, with addition of values from Olander 2004)

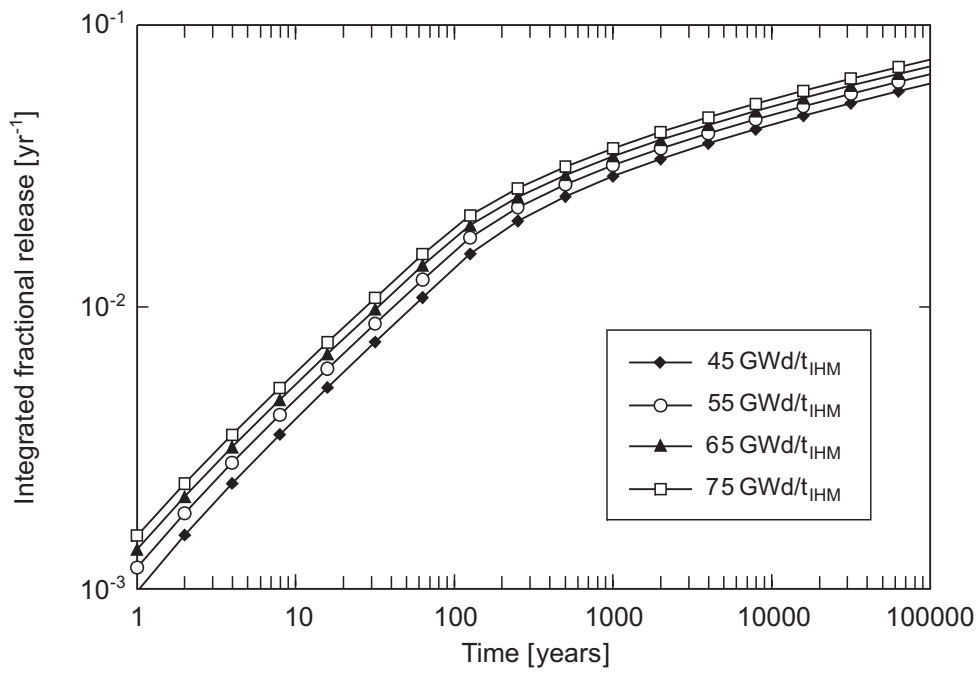


Fig. 4-3: Calculated released fraction from grains due to α self-irradiation enhanced diffusion for UO₂ fuels with burnups of 45, 55, 65 and 75 GWd/t_{IHM} (Lovera et al. 2003)

5 Experimental and Modelling Studies of Radiolysis and Effects of H₂

5.1 Radiolytic Modelling and Model Evaluation

Several radiolytic modeling studies were performed in the SFS Project, including comparison of model results with those from brine radiolysis experiments and with measured corrosion rates of UO₂ under various experimental conditions. The brine studies included sensitivity analyses for rate constants and G values for open and closed systems for gamma and for alpha radiation.

The substitution of molecular species (H₂ on the reducing side and H₂O₂ or HClO on the oxidizing side) by radicals can lower the H₂O₂ concentration by nearly three orders of magnitude. This is accompanied by formation of a steady state concentration for H₂ and O₂ (no further net decomposition of the solution).

The calculated production of radiolysis species in brine has been compared to a variety of experiments conducted under gamma and alpha irradiation. The standard deviation of results for gamma radiation experiments in an open system with respect to the formation rate of the molecular products H₂, O₂ and ClO₃⁻ is under most conditions (pH, concentration of Cl⁻ and contaminants) in the range of some 10 %. If contaminants are present the deviation between experimental and calculated concentrations is approximately the same. Only for Fe²⁺-containing solutions is the degree of agreement poorer. The comparison between experiments and calculation for the alpha radiolysis of brine with respect to H₂ and O₂ is similar to that for gamma radiolysis, but all chlorine species are underestimated from the calculation. The experimentally observed “protecting” effect of dissolved H₂ and the effect of added Br⁻ acting in the opposite direction are reasonably modeled. The deviation between experiments and calculation is for H₂ and in most cases for O₂ in the range of some 10 %.

5.2 Experimental Studies of UO₂ and SF Dissolution

Alpha-radiolysis Effects

A fundamental problem in assessing spent fuel dissolution rates in the long term is that no spent fuel that has decayed for thousands of years or more is available for experimental studies. As a result, experiments with spent fuel must be performed with fuel that has high beta-gamma emissions, whereas alpha-radiolysis is dominant after 1 000 years or more of decay. The effects of alpha-radiolysis of water on UO₂ dissolution can nonetheless be effectively explored by doping UO₂ with various levels of alpha-emitters to simulate fuels of different decay times. A large number of experiments with such doped materials have been performed under oxidising, anoxic and reducing (H₂ atmosphere) conditions. The activity of samples that have been prepared and studied in the SFS Project are compared in Figure 5-1 to the alpha-decay curves of spent fuels of various burnups. The samples allow alpha-radiolysis effects to be evaluated for equivalent decay times out to 10⁵ years.

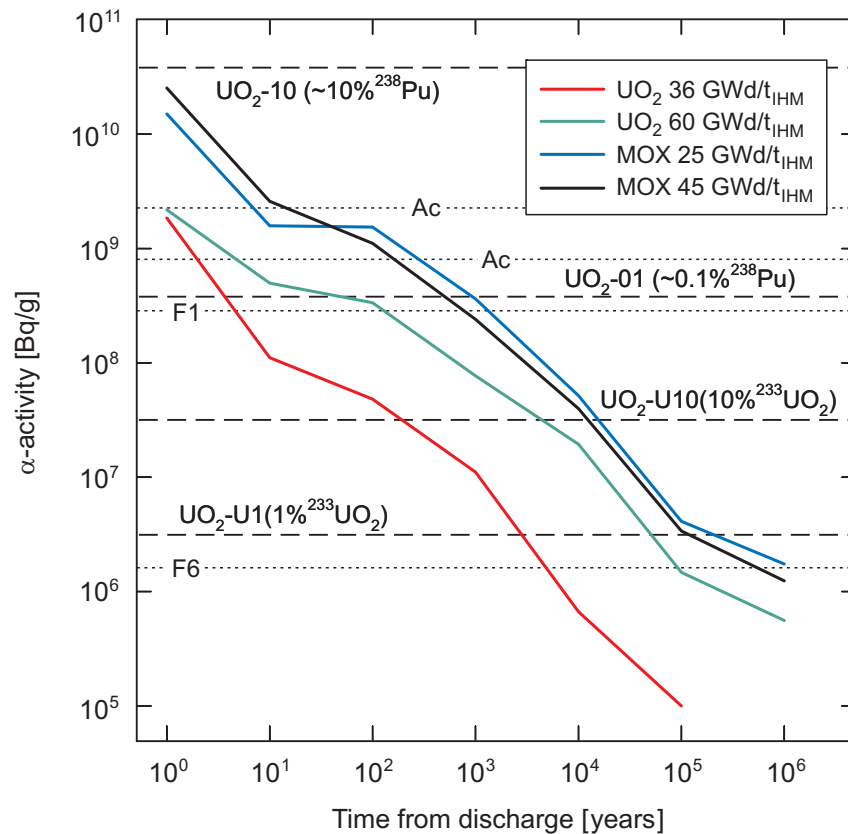


Fig. 5-1: Alpha-activity of various spent fuels as compared to the alpha activity of doped UO_2 samples used in the SFS Project

The results of various dissolution experiments show a clear trend of increasing corrosion rates with increasing specific alpha activity. An example is shown in Figure 5-2, from (Cachoir et al. in press), which shows U concentrations in deaerated solutions for UO_2 samples containing 0 %, 1 % and 10 % ^{233}U . In this example, it is clear that only the 10 % doped material experiences more significant dissolution than undoped UO_2 .

Based on a wide variety of such experiments, it can be concluded that there is generally a specific activity threshold below which no effect of alpha activity on dissolution rate is observed and above which an increase of corrosion rates with alpha activity is observed. The threshold activity probably depends on environmental parameters. It is about 37 MBq/g UO_2 in case of deaerated water (equivalent to a decay time of $\sim 10\,000$ years for a UO_2 fuel with a burnup of 60 GWd/ t_{IHM}). Below this threshold activity, the corrosion behaviour of unirradiated UO_2 or of a solid solution of UO_2 with representative fission product and actinide contents may adequately describe long term spent fuel matrix dissolution behaviour under anoxic conditions in which little or no H_2 is present.

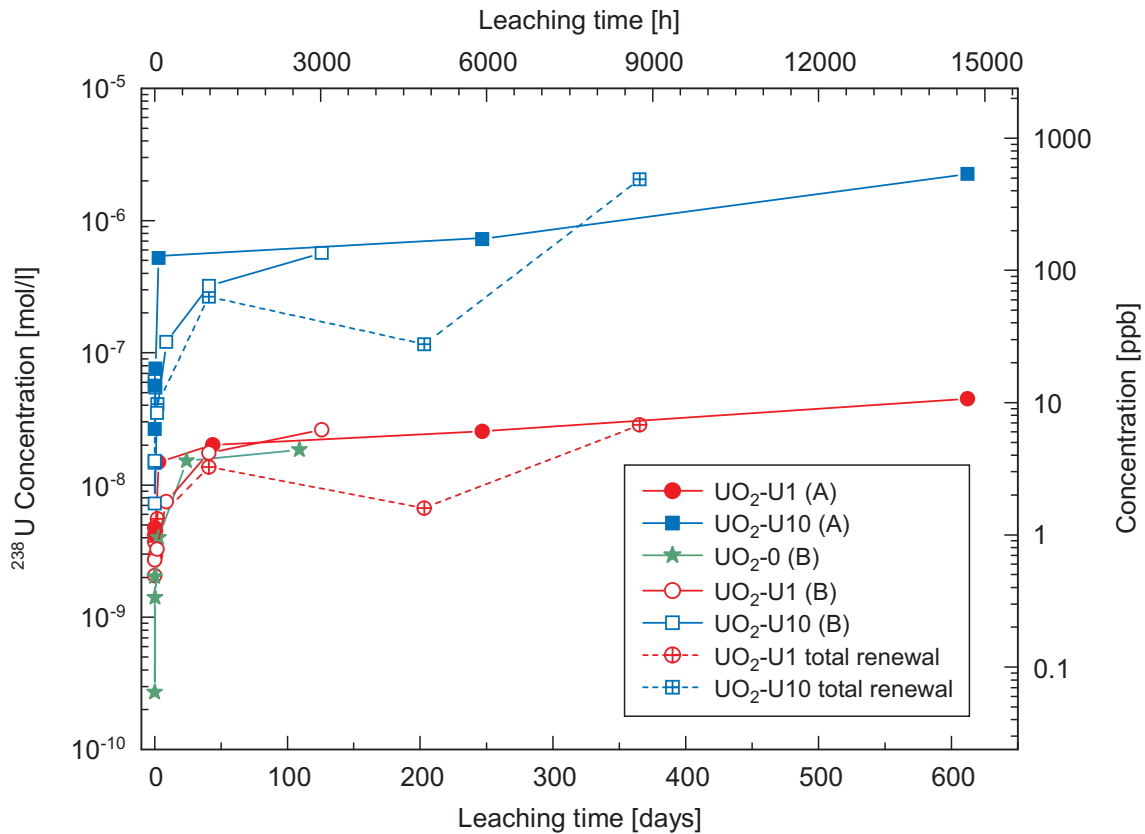


Fig. 5-2: Effects of alpha radiolysis on U dissolution under anoxic conditions: comparison of results from samples with no alpha-doping ($\text{UO}_2\text{-0}$), 1 % ^{233}U ($\text{UO}_2\text{-U}_1$) and 10 % ^{233}U ($\text{UO}_2\text{-U}_{10}$). Details are reported in Cachoir et al. (in press).

The effect of H_2 on the corrosion rate of alpha-doped UO_2 and spent fuel

As noted above, a clear enhancement in the uranium dissolution rate was observed for alpha-doped UO_2 samples in anoxic solutions above a certain threshold of alpha-activity. For experiments in the presence of $\text{Ar}/6\% \text{H}_2$ (total $P = 1$ bar), no further dissolution was observed after an initial dissolution up to an activity level of 10 % ^{233}U . These results can be contrasted with those from autoclave experiments, using samples with the same doping level, but with greater H_2 overpressures. Results from this experiment are shown in Figure 5-3 (Carbol et al. in press). Overpressures of H_2 were reduced stepwise from 16 bars to 0.01 bars over the duration of the experiment. Uranium concentrations in solution correspond to UO_2 in equilibrium with U(IV) . That no oxidation occurred was confirmed by XPS (X-ray photoelectron spectroscopy) performed at the end of the experiment. As can be seen in Figure 5-3, measured oxygen concentrations were at the detection limit and were far below values expected based on normal radiolytic yields.

These and other experiments performed with alpha-doped materials as well as with spent fuel provide a consistent picture suggesting that H_2 is an active reducing agent in these systems, which besides consuming oxygen arising from radiolysis and contamination from air, also reduces eventual traces of any U(VI) present. The explanation is thought to be activation of the H_2 at the irradiated UO_2 surface. Future development of any matrix alteration model should attempt to incorporate such surface processes.

Although there is more work to be done to clearly understand the effects of H₂, the experimental data obtained in this project together with literature data give a reliable foundation to use alteration/dissolution rates for spent fuel of the order of 10⁻⁶/yr-10⁻⁸/yr, with a recommended value of 4×10⁻⁷/yr for dissolved hydrogen concentrations above 10⁻³ M and Fe(II) concentrations typical for European repository concepts. These estimates are independent of those made using the MAM, which calculates dissolution rates based on a radiolytic model described in Section 6

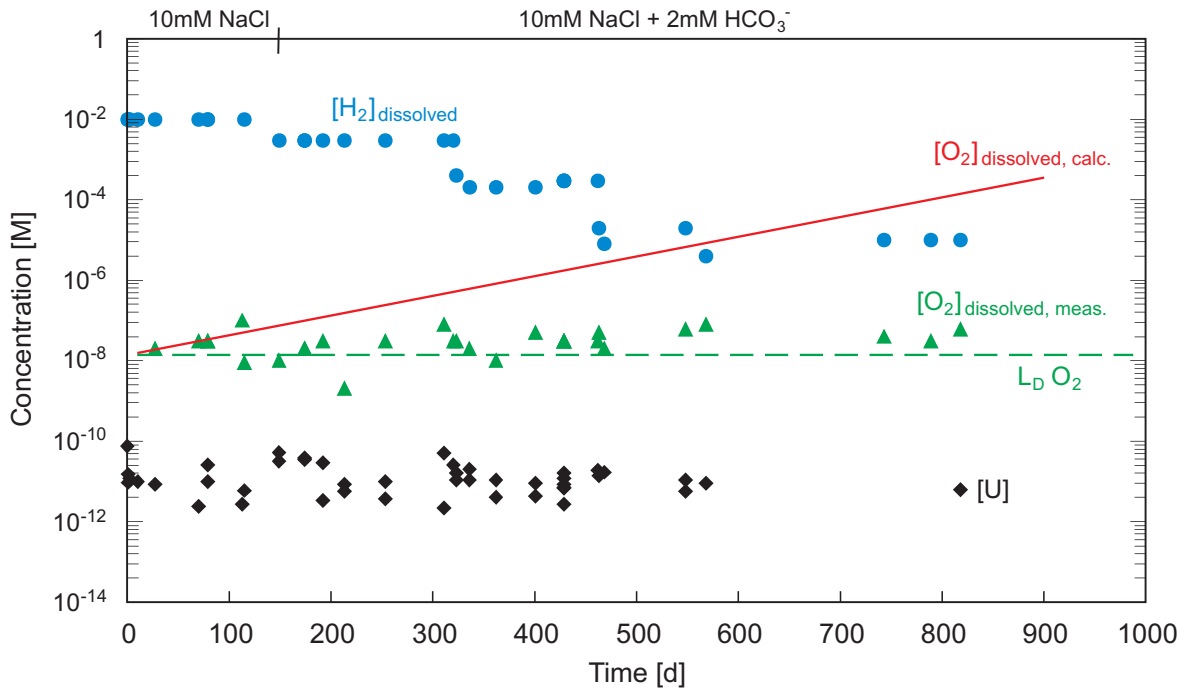


Fig. 5-3: Measured total U and H₂ concentrations in solution in contact with UO₂ doped with 10 % ²³³U (details are discussed in Carbol et al. (in press).

6 The Matrix Alteration Model (MAM)

6.1 Overview

The conceptual model underlying the MAM incorporates the following processes affecting the oxidation and dissolution of the spent fuel matrix:

- *Process 1.* Generation of oxidants and reductants by water radiolysis.
- *Process 2.* Oxidation of the spent fuel.
- *Process 3.* Reduction of the oxidants present in the system.
- *Process 4.* Dissolution of the matrix.

In order to quantify the amount of species generated radiolytically, as well as the rate of alteration of the spent fuel matrix, the model integrates the processes described above as follows:

- Generation and recombination of radiolysis products; i.e. the generation of molecular and radical oxidants and reductants and their recombination reactions.
- Spent fuel surface alteration processes; i.e. consumption of oxidants by the spent fuel surface in the overall balance of the species generated radiolytically.

Kinetic parameters as well as the reaction mechanisms have been elucidated partly from the models developed based on non-irradiated uranium dioxide dissolution experiments (de Pablo et al. 1999, Giménez et al. 2001, de Pablo et al. 2003 & de Pablo et al. 2004). In addition, the reaction mechanisms and kinetic constants determined in the work performed by Ekeröth & Jonsson (2003) with hydrogen peroxide have also been relevant for determining the surface alteration processes. The surface area of spent fuel is assumed to be 70 cm²/g, based on the BET measurements of Forsyth (1997), about ten times higher than the geometric surface area of spent fuel fragments. The potential evolution of surface area through processes such as secondary phase formation, which might reduce the effective surface area or microcracking at grain boundaries due to He buildup, which might increase surface area, has not been considered in the calculations, due to insufficient data. It has not been possible to fully incorporate the surface effects of H₂ on dissolution rate (see Section 5), although these aspects are partially simulated through the calculation of oxidant production in solution with the radiolytic model (i.e. scavenging of oxygen and peroxide production) when high hydrogen pressures are applied.

6.2 Validation of the MAM

Results from a wide variety of experiments involving UO₂ dissolution have been compared to MAM predictions, with generally good agreement. One example is shown in Figure 6-1, which illustrates the good correspondence between MAM predictions and measured dissolution rates over a broad range of pH values at a hydrogen peroxide concentration of 10⁻⁵ mol l⁻¹ (Merino et al. in press).

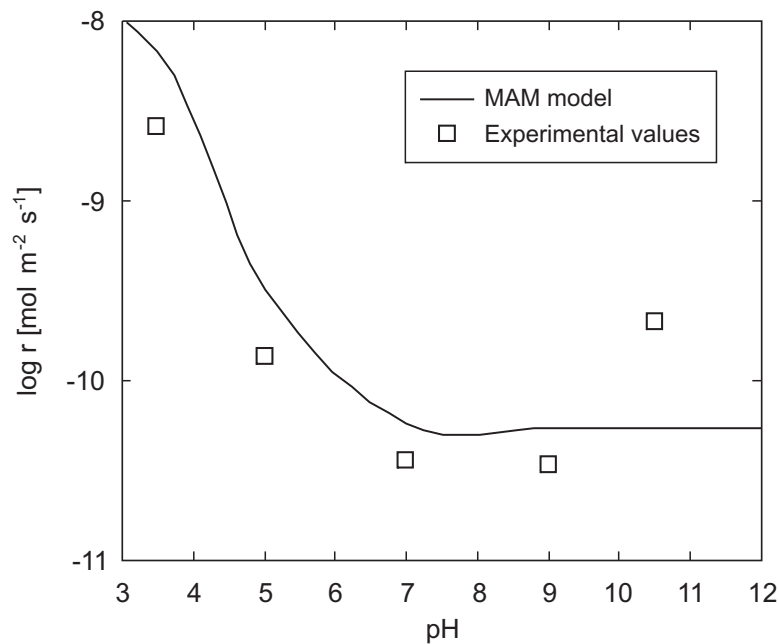


Fig. 6-1: UO_2 dissolution rate calculated using the MAM model compared to results from flow-through experiments with unirradiated UO_2 at various pH values with $[\text{H}_2\text{O}_2] = 1 \times 10^{-5}$ M. See Merino et al. (in press) for details.

In cases involving H_2 overpressures, it has proven difficult to test the model, as uranium concentrations do not increase with time, suggesting additional processes beyond those incorporated in MAM are occurring. These aspects are discussed in Section 5.2.

6.3 Time-dependent Calculations Using the MAM for the Granite and Clay Cases

The MAM was used to calculate time-dependent concentrations of molecular oxidants and reductants and fuel dissolution rates over the period from 10^3 to 10^6 years (Figure 6-2). This extrapolation was performed assuming that the waste container failed at 1000 years. The reference burnup of the spent fuel for the base case calculation was $41.5 \text{ GWd/t}_{\text{HM}}$, with a geometry consisting of a fuel pellet surrounded by a gap full of water. In both cases, a constant H_2 pressure of 3 bars arising from container corrosion was assumed. For more details on boundary conditions, geometry, parameters and kinetic reactions see the conceptual model report (Martínez-Esparza et al. 2005). Alpha dose rate evolution takes into account the inventory of the reference fuel (alpha activity is dominated by the isotopes of Pu, U, Cm and Am), the self-absorption of alpha particles in the spent fuel itself and their range in water and the energy deposited in the water in the fuel/sheath gap.

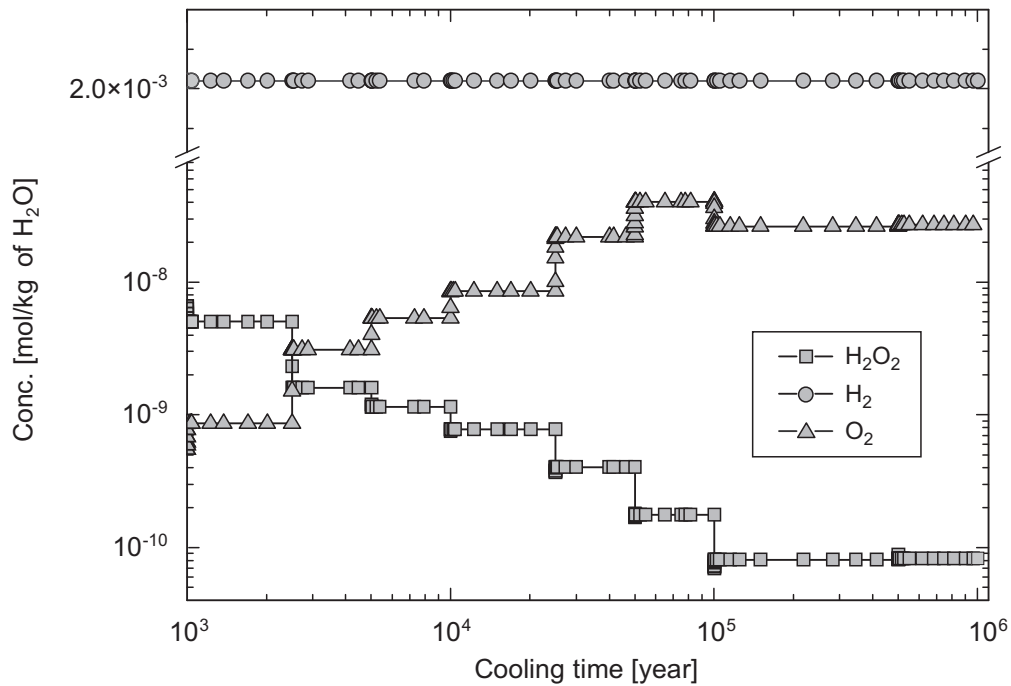


Fig. 6-2: Evolution of the molecular species concentrations in solution in granite reference case

The MAM predictions of the dissolution rate for the base case fuel for both granite and clay porewaters are shown in Figure 6-3. There are small differences between the two cases arising from different carbonate and pH conditions.

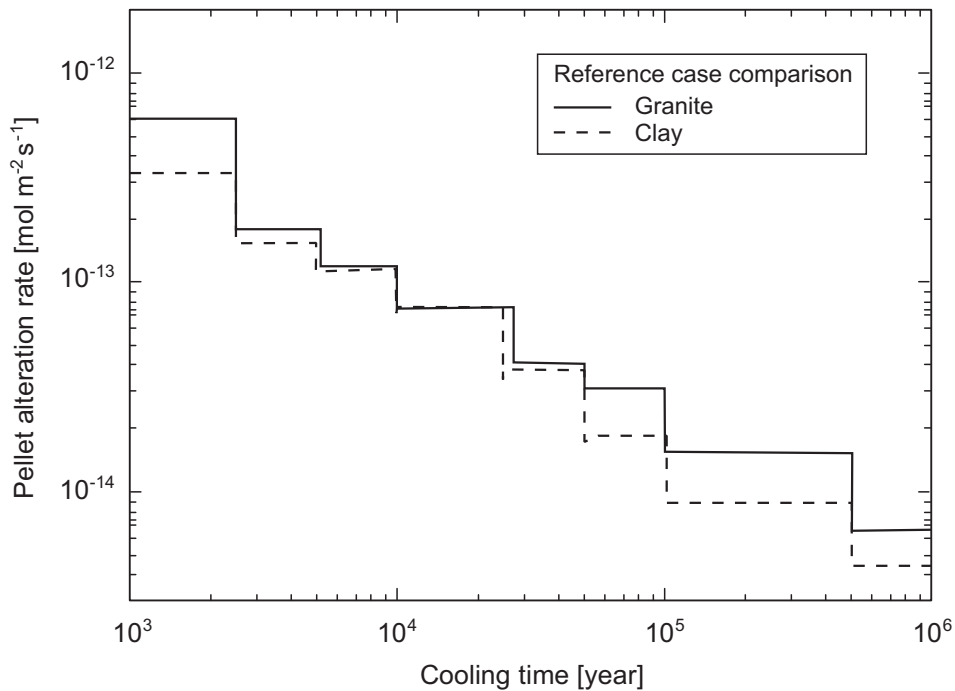


Fig. 6-3: Time-dependent alteration rate calculated with the MAM for spent fuel (burnup = 41 GWd/t_{IHM}) in granite and clay porewaters

6.4 Application of MAM to Salt Repository Conditions

The radiolytic calculation scheme used in MAM appears to underestimate the spent fuel corrosion rate in brine solution likely because no oxidation reaction exists in the model between the chlorine species and the UO_2 matrix. If a reaction between Cl_2^- and UO_2 is added to the reaction scheme, a rate constant can be inferred by fitting the model dissolution rate curve to the measured dissolution rate data. The revised reaction scheme including the new reaction has been used to calculate the initial dissolution rate ($t = 1\ 000$ years) and the values for granite, clay and brine are compared in Table 6-1.

Tab. 6-1: Comparison of spent fuel dissolution rates at 1 000 years for granite, clay and salt porewaters

Medium	Water chemistry	Radiolytic yields	Surface area	UO_2 alteration scheme	r ($\text{mol m}^{-2} \text{s}^{-1}$)
Granite	$2 \times 10^{-3} \text{ M HCO}_3^-$, 0.01 M Cl^-	water	specific ($70 \text{ cm}^2 \times \text{g}^{-1}$)	<i>no Cl_2^- reaction</i>	5.70×10^{-13}
Clay		water	specific ($70 \text{ cm}^2 \times \text{g}^{-1}$)	<i>no Cl_2^- reaction</i>	3.2×10^{-13}
Salt	<i>5 M Cl⁻, no CO₃'s</i>	brines	specific ($70 \text{ cm}^2 \times \text{g}^{-1}$)	<i>with the Cl_2^- reaction</i>	7.70×10^{-13}

Additional calculations were performed using other radiolysis schemes for brine solutions. These schemes, which include chloride species, result in rates (at 1 000 a) of 8×10^{-13} to $1 \times 10^{-12} \text{ mol m}^{-2} \text{ s}^{-1}$, slightly higher than values for clay and granite waters. The latter value has been used as a basis to extrapolate with time based on the decay curve of the reference fuel. Based on the time-dependent rates of dissolution for the reference case spent fuel ($41.5 \text{ GWd/t}_{\text{HM}}$) for the three reference groundwaters, the fraction of the fuel altered as a function of time has been calculated and this is illustrated in Figure 6-4. The relative increase in fraction altered for granite groundwater compared to the other two cases likely arises because detailed evolution of chemistry (pH and carbonate, in particular) is accounted for in the former but not in the latter.

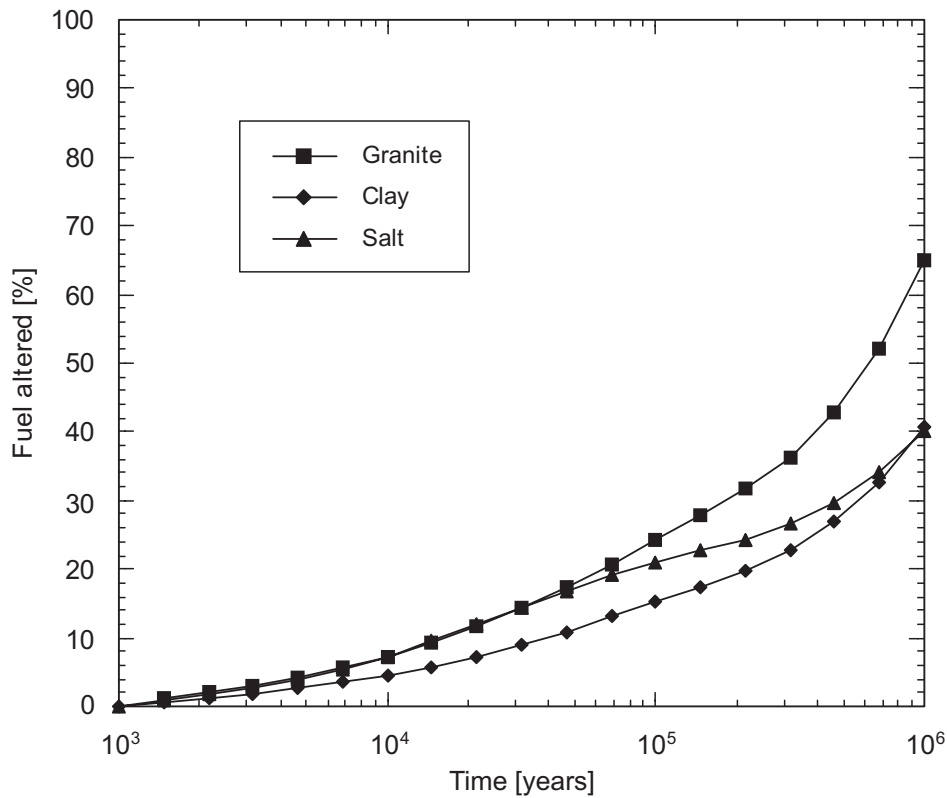


Fig: 6-4: Fraction of reference spent fuel (burnup = 41 GWd/t_{IHM}) altered as a function of time in the three reference groundwaters (granite, clay, salt brine), calculated using the MAM.

6.5 Overview of the Integrated Model for Spent Fuel Dissolution

The Integrated Model for spent fuel dissolution combines the IRF model and the MAM to calculate time-dependent releases from a hypothetical container with 1 t_{IHM} of spent fuel, using the SPENT code (Nagra 2002a), with some code modifications specific to the SFS Project. The conceptual model is illustrated in Figure 6-5.

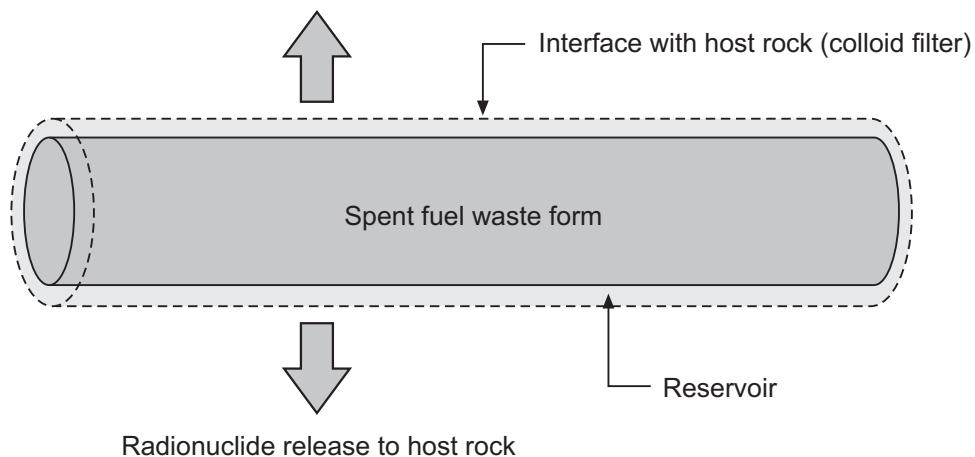


Fig. 6-5: Illustration of the conceptual model used in the Integrated SFS Model

Although strictly speaking, aspects such as radionuclide solubilities after release from spent fuel and mass transport are not typically part of a process model for radionuclide release, they are essential in the implementation of any performance assessment-based model for the process. As a result, it is worthwhile to integrate all these phenomena to explore their combined effects on release from a canister of spent fuel.

The following processes are modelled:

- complete containment of radionuclides is assumed up to a container breaching time of 1 000 years,
- following breaching, the IRF, which includes the amounts from time dependent solid-state diffusion, is released to a water-filled void space in the container,
- the transport resistance of the breached container is neglected (note that this assumption is made for all cases for reasons of simplification and comparison of results; in some assessments, release from a very small defect is shown to have a large effect on release from the container),
- release from the fuel matrix begins using the time-dependent values obtained with the MAM,
- radionuclide concentrations in the reservoir are constrained by solubility limits for the respective elements,
- release from the container is constrained by the rate of fluid flow at the buffer / host rock interface (to avoid complications related to sorption on a buffer material, no buffer is present in the model), thus radionuclides are transferred directly from the reservoir solution to the host rock; however, any colloids generated in the reservoir due to solubility limits being exceeded do not migrate into the rock, but rather remain within the reservoir until concentrations there fall and they redissolve.

The derivation of the equations for the transport conditions for the release model is given in Appendix 1. Based on this derivation, the effective flow rate Q_{eff} at the boundary with the host rock can be specified according to:

$$Q_{eff} = 2a \left[6q_{HR} + \frac{\pi D_{HR}}{L_{HR}} \right]$$

where

L_{HR} is a length scale characterising the diffusive transport distance across the host rock (e.g. the thickness of the host formation).

D_{HR} is the effective diffusion coefficient of the host rock,

a is the near-field tunnel radius (assuming in-tunnel emplacement) and

q_{HR} is the Darcy velocity in the rock,

Three types of host rock are considered, namely (i), a fractured crystalline rock, (ii), a homogeneous clay sediment and (iii), salt. Selected parameter values are presented in Table 6-2.

Tab. 6-2: Parameter values relevant to mass transport at the interface between the near field and the host rock

Parameter	Crystalline	Clay	Salt
D_{HR} [m ² /a]	0	3.2×10^{-4} (10^{-11} m ² /s)	10^{-12} m ² /s
L_{HR} [m]	-	40	500
q_{HR} [m/a]	2×10^{-3}	6.4×10^{-7} (2×10^{-14} m/s)	0
a [m]	1.25	1.25	3
Q_{eff} [m ³ /a per m length of container]	3×10^{-2}	7.2×10^{-5}	1.2×10^{-6}

For the fractured crystalline rock, transport at the near field / host rock interface is assumed to be advection dominated, $D_{HR} = 0$. The Swedish SR 97 safety assessment gives „reasonable” values for the q_{HR} at the hypothetical Aberg, Beberg and Ceberg sites as 2×10^{-3} , 10^{-3} and 4×10^{-5} m/a, respectively (SKB 1999). For the present study, it is proposed to take the highest of the three, i.e. the value for Aberg. A tunnel radius of 1.25 m is taken from Nagra’s Opalinus Clay study (Nagra 2002b), with a 40 m rock layer half-thickness considered to be a typical minimum value for a sedimentary formation.

For sediment, transport parameter values are taken from Nagra’s Project Opalinus Clay safety assessment (Nagra 2002b). Note that values from Callovo-Oxfordian and Boom Clay formations will give very similar Q_{eff} values to the one derived for Opalinus Clay.

Table 6-3 gives the data inputs for the fuel and container. Radionuclide solubilities are taken from previously published studies. It is assumed that the effective flow rate per waste package can be obtained by multiplying Q_{eff} by the waste package length, i.e. the space between waste packages is neglected for the purposes of the present study.

Tab. 6-3: Fuel and container parameters

Parameter	Crystalline	Sediment	Salt
RN solubilities	SR-97 values (SKB 1999)	Nagra (2002a)	Metz (private communication, SFS Project)
Void volume in container (reservoir volume)	0.5 m ³	0.5 m ³	0.5 m ³
Container length	5 m	5 m	5 m
Fuel inventory in container	PWR (1 t _{IHM})	PWR (1 t _{IHM})	PWR (1 t _{IHM})
Radionuclide inventories in fuel	Provided by CEA for BU = 33, 41, 48, 60 GWd/t _{IHM} Poinssot (personal communication)	Provided by CEA for BU = 33, 41, 48, 60 GWd/t _{IHM} Poinssot (personal communication)	Provided by CEA for BU = 33, 41, 48, 60 GWd/t _{IHM} Poinssot (personal communication)
IRF (t = 0) values	Tables 4-1 and 4-2		

Some calculations with the Integrated Model have been performed to illustrate various aspects of spent fuel behaviour and of the release of radionuclides from a container with 1 t_{IHM} of spent fuel. These are presented in Section 7.4 and illustrate the combined processes of:

- instant release into the reservoir in the container when breaching occurs,
- dissolution of the spent fuel matrix
- transport controlled release from the container,
- accumulation in the precipitate (and gradual precipitate dissolution) within the container for low solubility nuclides,
- radioactive decay

7 Spent Fuel Evolution Over Time: Performance Assessment Perspectives

7.1 Introduction

The experimental and modelling studies performed within the SFS Project provide a valuable basis for illustrating the significance of various phenomena associated with the evolution of spent fuel in geological repositories. These aspects are examined here through various illustrative calculations and discussion, including:

- comparison of the range of alteration rates calculated with the MAM for different groundwaters with the possible range of values derived from studies of the effect of H₂ on alteration rates,
- time-dependent alteration rates of fuel for different burnup values, using the MAM
- illustration of radionuclide release rates combining IRF (t = 0), IRF (t)¹ and matrix dissolution
- results from an integrated dissolution model (described in Section 6.5), which combines the IRF model with the MAM and calculates rates of release from a hypothetical container with 1 t_{IHM} of spent fuel, for different burnup and groundwater chemistry conditions and
- discussion of progress made relative to previous models and of remaining uncertainties relevant to future model development.

7.2 Comparison of alteration rates calculated using the MAM with experimentally-derived rates for H₂-dominated systems

As discussed in Section 5.2, based on studies of spent fuel dissolution and alpha-radiolysis effects on UO₂ dissolution in H₂-dominated systems, it is possible to estimate a range of fuel dissolution rates under conditions in which H₂ appears to be an active reducing agent. The rates proposed in Section 5.2 for such conditions are compared to rates calculated with the MAM (converted to fractional dissolution rates) for the three groundwaters in Figure 7-1. The absence of any time-dependence (dose-rate dependence) for H₂-dominated systems may or may not be real, and further work should be done to assess this aspect.

¹ See Section 7.4

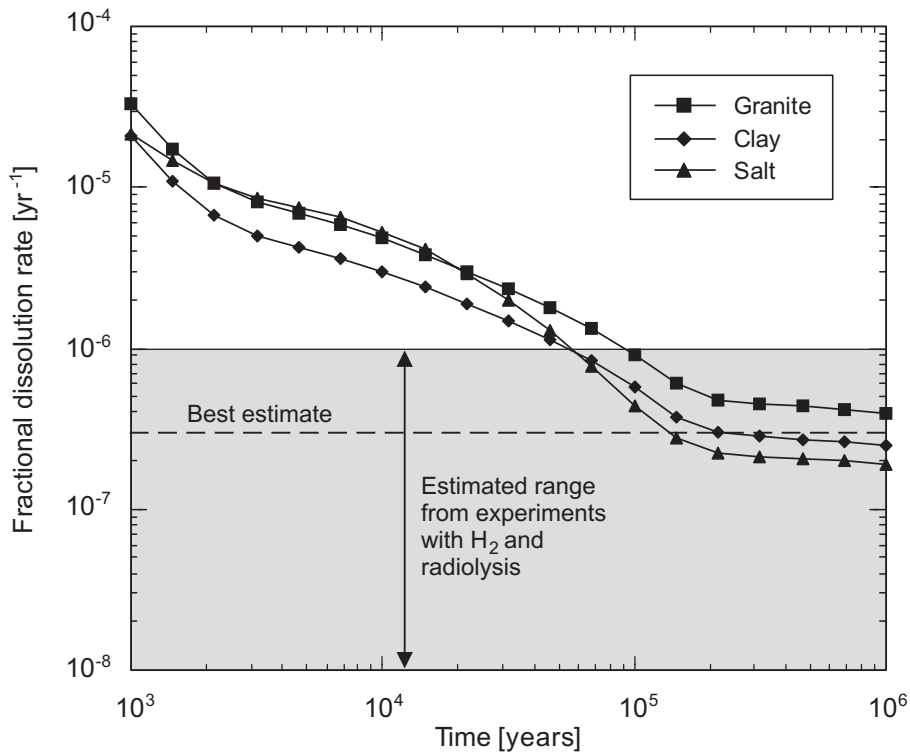


Fig. 7-1: Comparison of fractional dissolution rates calculated using the MAM with the range of values estimated from experimental studies of dissolution of alpha-doped UO₂ and spent fuel in the presence of H₂

7.3 Influence of Burnup and Container Breaching Time on SF Dissolution Rates Calculated with the MAM

Alteration rates calculated with the MAM are, of course, dependent on the dose rate, thus MAM calculations show a difference in time-dependent alteration rate depending on the fuel burnup, in particular at early times. This is illustrated in Figure 7-2 for burnup values ranging from 33 to 60 GWd/t_{IHM}. As seen in Figure 7-3, this leads to differences in the integrated fraction of fuel altered of about 5 % at 10⁵ years. Such an effect would be even more pronounced with MOX fuel; however, no estimates of the matrix dissolution rate have been made for MOX fuel using the MAM, as little data is available to support the validity of such calculations.

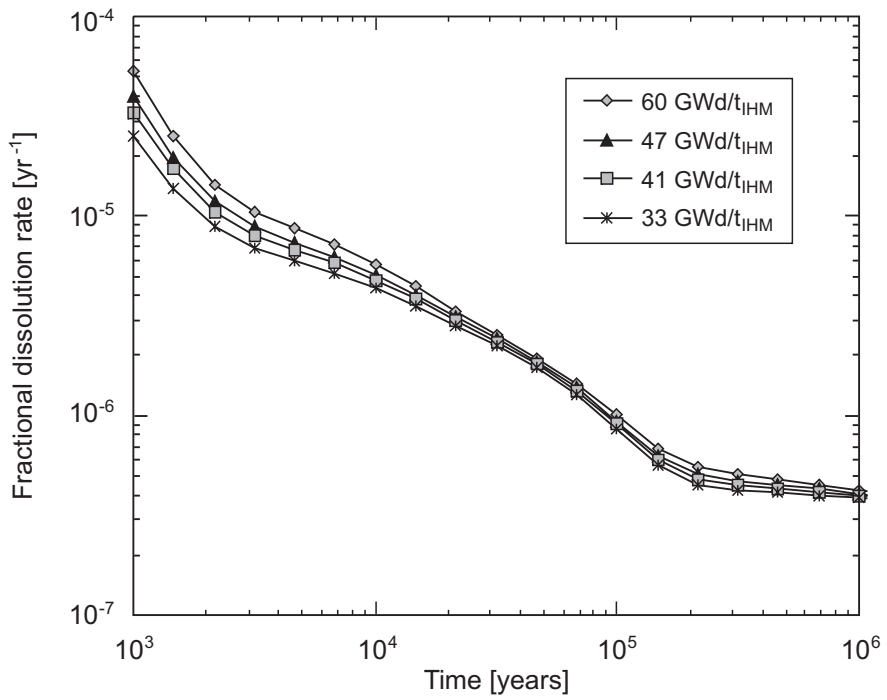


Fig. 7-2: Effect of fuel burnup on fuel alteration rate as calculated with the MAM

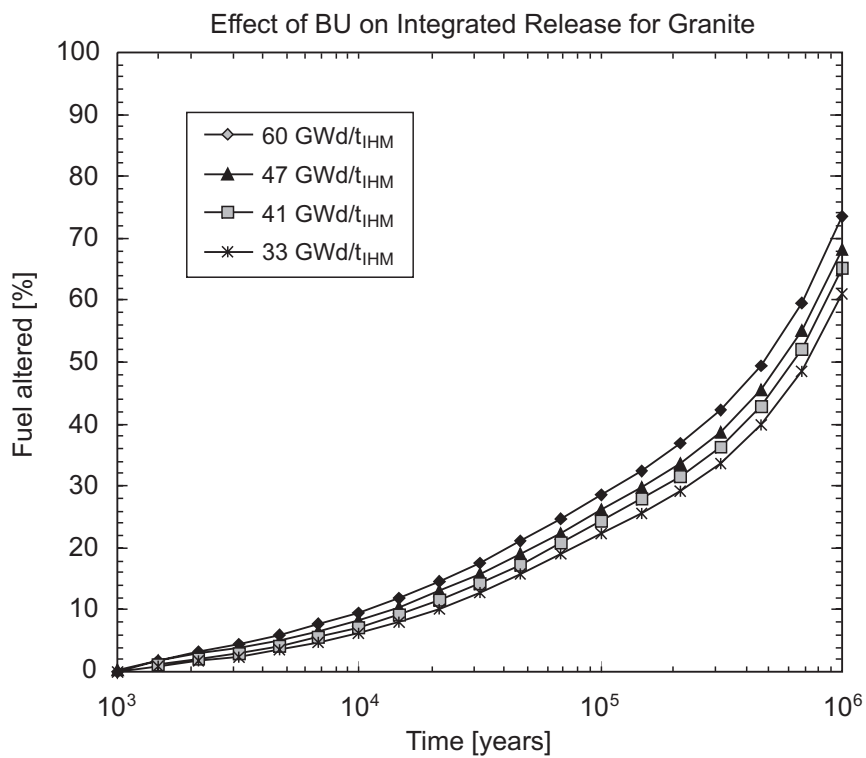


Fig. 7-3: Effect of burnup on fraction of fuel altered over time for granite groundwater

The effect of container breaching time on the integrated fraction altered is also of interest. In the SFS Project, a reference container breaching time is considered for all calculations. However, there is an expectation of significantly longer lifetimes. As expected, given the dependency of the alteration rate on alpha activity, longer lifetimes lead to a significant decrease in the fraction altered, e.g. about 24 % (1 000 year breaching) vs. 16 % at (10 000) year breaching) after 10^5 years, as shown in Figure 7-4. Whether or not this would actually be the case is not clear, as the time-dependency of the rate may be much less important under high hydrogen pressure conditions (see Figure 6-5). Note that the IRF in Figure 7-4 represents only the $t = 0$ contribution – the time-dependent contribution is discussed in Section 7.4

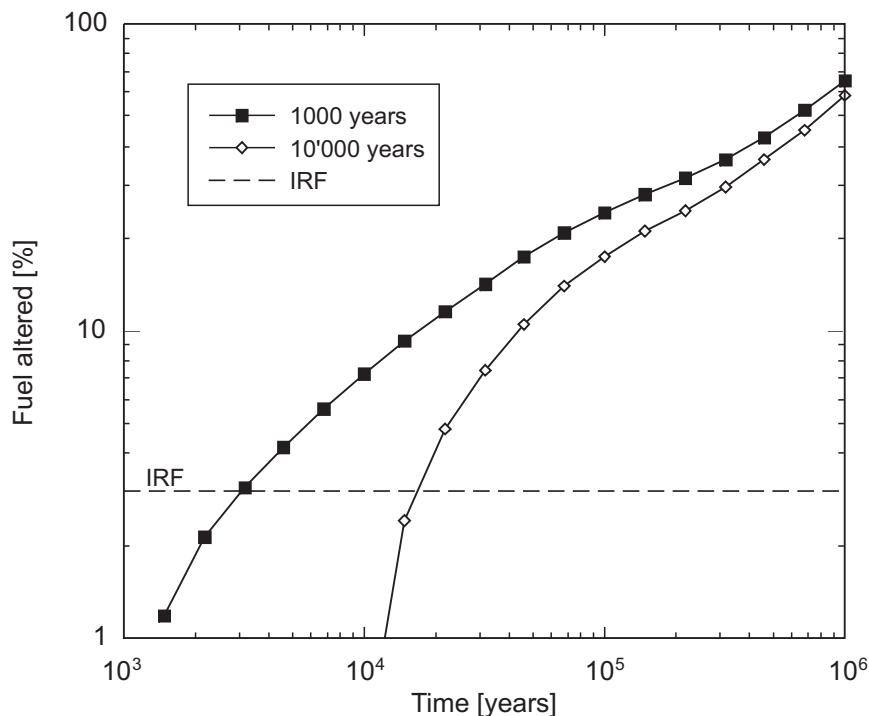


Fig. 7-4: Effect of canister breaching time on the time-dependent alteration rate as calculated with the MAM (granite case), for a fuel burnup of $41 \text{ GWd}/t_{\text{IHM}}$. Only the IRF at $t = 0$ is shown here.

7.4 Relative contributions of IRF, Alpha-enhanced Diffusion and Matrix Dissolution to Radionuclide Release

It is interesting to compare the relative contributions of the IRF (i.e. IRF $t = 0$), alpha-enhanced solid state diffusion (i.e. IRF (t)) and matrix dissolution to radionuclide release for different burnup values. (Note that the term IRF (t) used here refers only to the time-dependent portion of the IRF.) The relative contributions can be seen in Figures 7-5 and 7-6 for spent fuel with burnup values of 41 and $60 \text{ GWd}/t_{\text{IHM}}$. In Figure 7-5, it can be seen that the IRF ($t = 0$) is relatively low at 3 % and that the additional contribution to release of radiation-enhanced diffusion using the upper curve in Figure 4-2 is about 5 % at 10^5 years. For a burnup of $60 \text{ GWd}/t_{\text{IHM}}$, the IRF ($t = 0$) is much larger (~ 12 %) and the time-dependent contribution is about 7 %. Calculations illustrate that if the time-dependent diffusion coefficient is about one order of magnitude lower than that assumed in Figures 7-5 and 7-6, this process will contribute little to radionuclide release, thus it would be useful to develop some approach that permits discriminating between the alternative models in Figure 4-2.

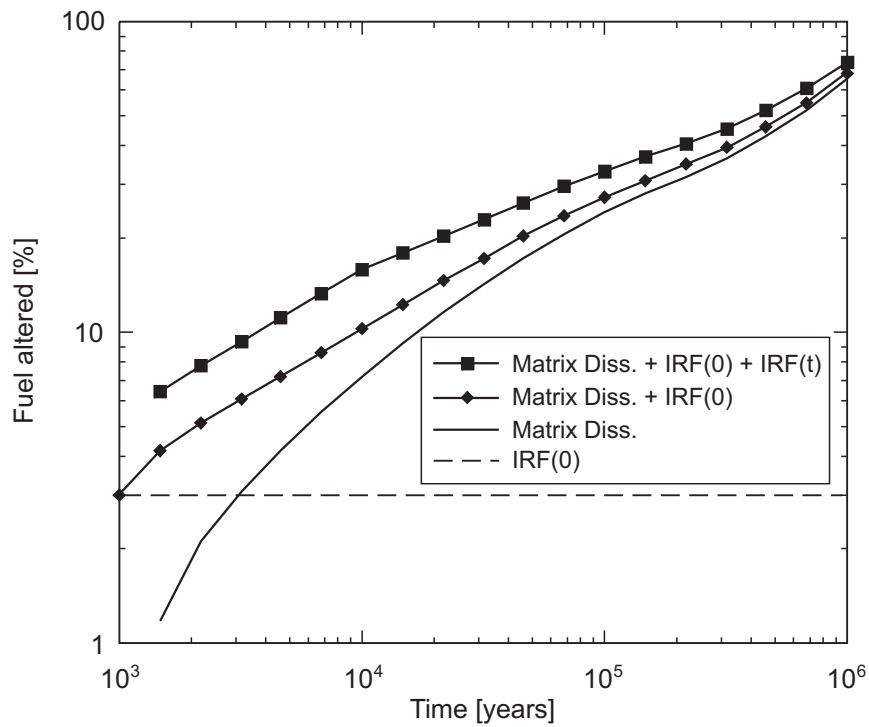


Fig. 7-5: Integrated release of I-129 from spent fuel with a burnup of 41 GWd/ t_{IHM} (granite case) considering matrix dissolution only (lower curve), matrix dissolution plus IRF ($t = 0$) and matrix dissolution plus IRF ($t = 0$) plus IRF (t).

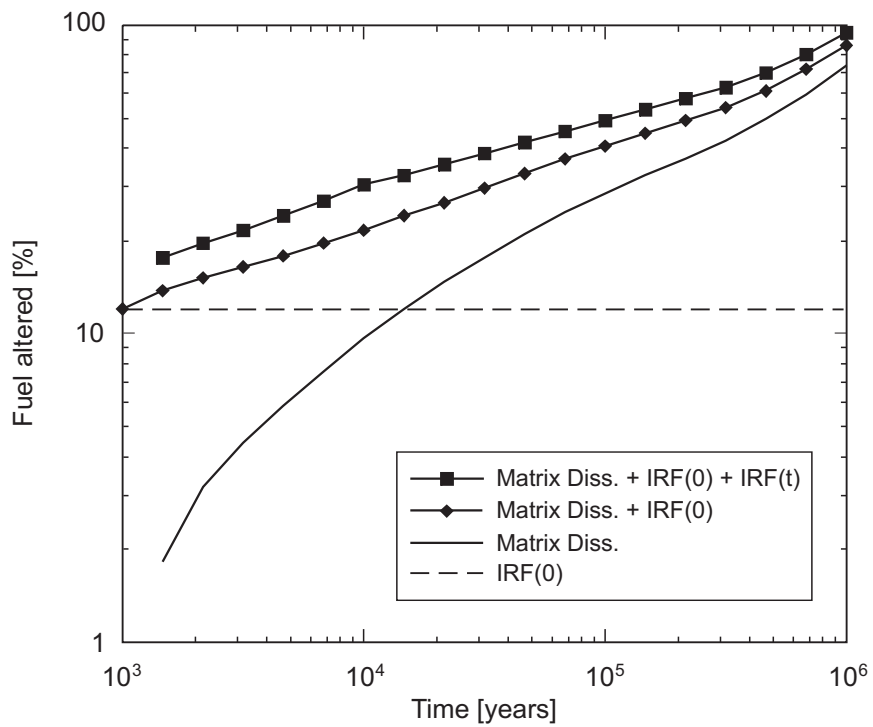


Fig. 7-6: Integrated release of I-129 from spent PWR fuel with a burnup of 60 GWd/ t_{IHM} (granite case), considering matrix dissolution only (lower curve), matrix dissolution plus IRF ($t = 0$) and matrix dissolution plus IRF ($t = 0$) plus IRF (t).

7.5 Results of calculations using the integrated model for radionuclide release from spent fuel

The integrated model (see Section 6.4) combines the IRF model, the MAM, nuclide solubilities and near-field mass transport rates to illustrate the time-dependent release of radionuclides from a reference canister of spent fuel ($1 t_{IHM}$). The distribution of I-129 in the disposal system as a function of time for fuel with a burnup of $41 \text{ GWd}/t_{IHM}$, as calculated with the integrated model, is shown in Figure 7-7 for granite repository porewater chemistry and mass transport conditions. When the container is breached at 1 000 years, the IRF is released into the void space within the container and begins to be released into the surrounding rock (note there is no transport limitation due to the residual container – see Figure 6-5). After about 500 000 years, the fraction of the total initial inventory that is released from the container is about 50 %. Dissolution and release from the canister is complete after about 1.5 M years.

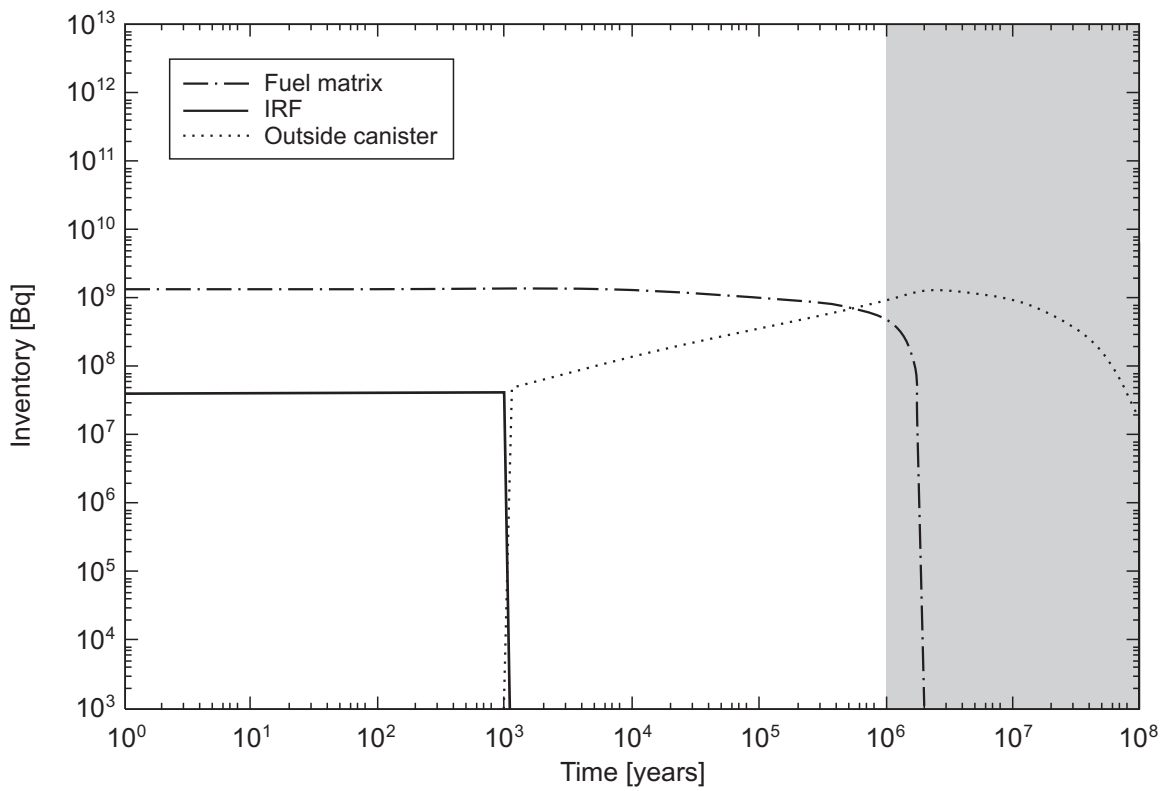


Fig. 7-7: The distribution of I-129 as a function of time, showing the amounts in the fuel matrix, IRF and released from the container, for fuel with a burnup of $41 \text{ GWd}/t_{IHM}$

In Figure 7-8, the distribution of Pu-239 is shown, again for granite repository conditions. In this case, a precipitate forms quickly due to the large amount of Pu released from the matrix compared to the low solubility of Pu (7×10^{-9} mol/l). This greatly limits the release from the container. The Pu-239 decays away well before dissolution of the matrix or precipitate is complete, thus only a very small fraction of the initially large Pu inventory is actually released from the container.

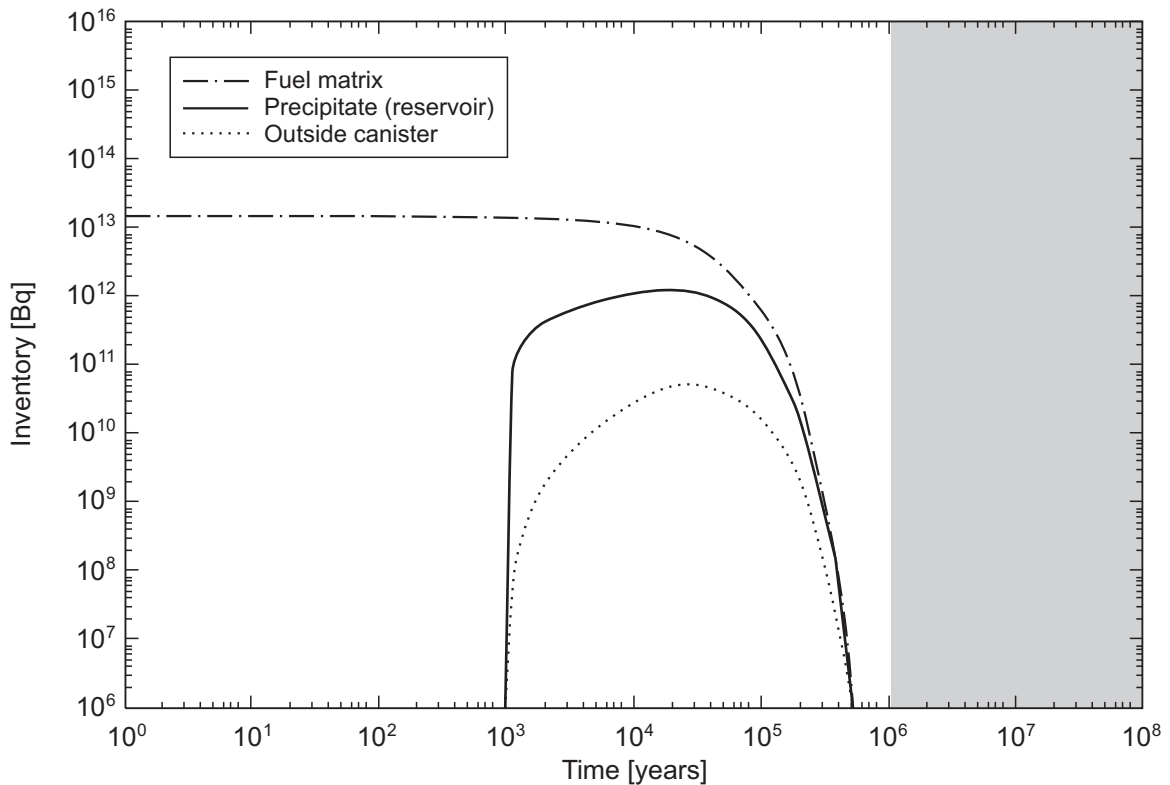


Fig. 7-8: The distribution of Pu-239 as a function of time, showing the amounts in the fuel matrix, precipitate within the container (solubility = 7×10^{-9} mol/l) and released from the container, for a fuel burnup of 60 GWd/ t_{HIM} (granite case).

In Figure 7-9, the release behaviour of I-129 is compared for reference containers of spent fuel (1 t_{HIM} with a burnup of 41 GWd/ t_{HIM}) in clay, granite and salt repository conditions. Because there is no solubility limit, releases from the containers are very similar in all three cases, despite the significantly different mass transport conditions (see Table 6-2). This is in contrast to the case shown in Figure 7-10 for Np-237, where a precipitate forms. Here the relatively higher mass transport rate from the container under granite repository (Np solubility = 6×10^{-8} mol/l) conditions leads to less accumulation in the precipitate and to its earlier dissolution, as compared to the clay (Np solubility = 5×10^{-9} mol/l) and salt (Np solubility = 3×10^{-7} mol/l) repository cases. These results illustrate that release from spent fuel and the associated precipitates under disposal conditions is a complex function of matrix alteration rate, nuclide solubility and mass transport conditions.

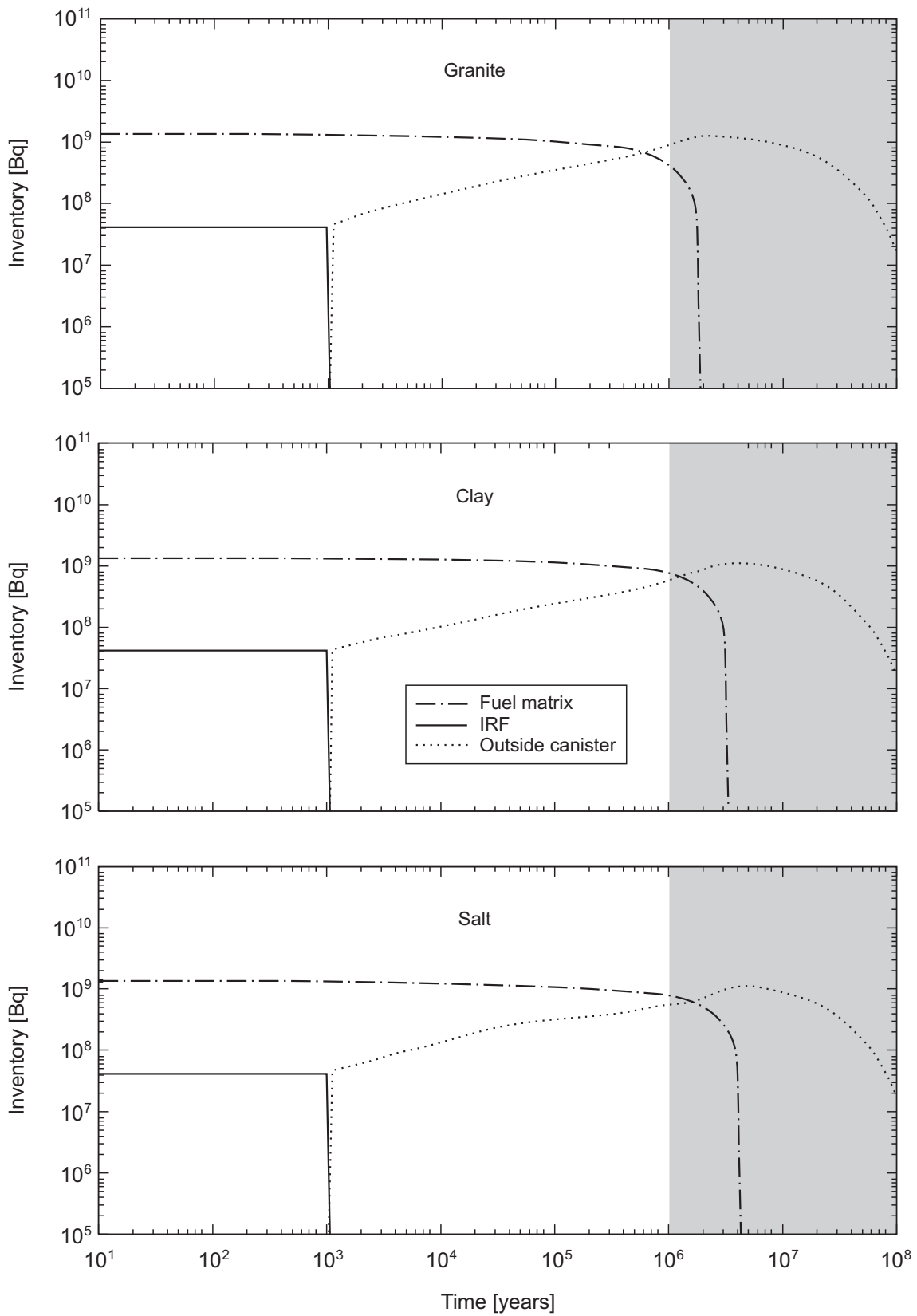


Fig. 7-9: The distribution of I-129 as a function of time for the case of containers of spent fuel (burnup = 41 GWd/t_{IHM}) having breaching times of 1 000 years in repositories in granite, clay and salt

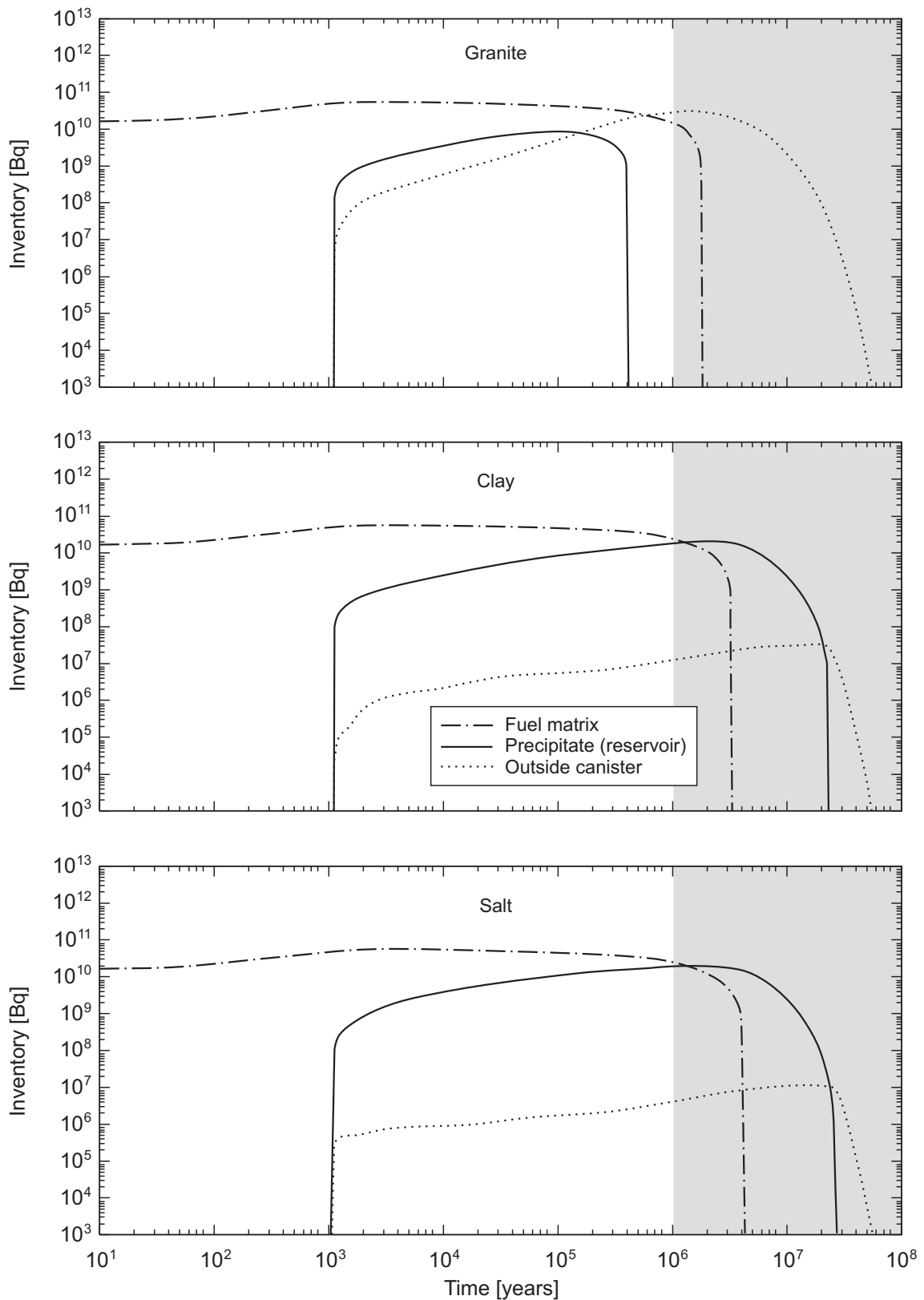


Fig. 7-10: The distribution of Np-237 as a function of time for the case of containers of spent fuel (burnup = 41 GWd/ t_{THM}) having a breaching time of 1 000 years in repositories in granite, clay and salt

8 Summary

The SFS Project has developed a model for radionuclide release from spent fuel that is relevant to conditions in repositories in granite, clay and salt host rocks. The model is based on the following main elements:

- review of existing databases on fission gas release and short-term leaching behaviour of various radionuclides to establish the Instant Release Fraction (IRF) at the time of discharge from reactor, for both UO_2 and MOX fuels for a wide range of burnups,
- modelling of solid state diffusion processes that may lead to further transport of some radionuclides to grain boundaries, leading to a model for a time-dependent component of the IRF,
- development and validation of a fuel matrix alteration model (MAM), based on time-dependent production of radiolytic species coupled to oxidative dissolution, evaluated under the conditions of elevated H_2 pressure in a repository,
- radiolytic modelling and validation experiments in salt brines for both alpha and gamma radiolysis,
- extensive studies of the dissolution of alpha-doped UO_2 and spent fuel covering a broad range of redox conditions,
- assessment of the effects of hydrogen on the dissolution of alpha-doped UO_2 and spent fuel,
- integration of the MAM and IRF models to illustrate the behaviour of spent fuel in granite, clay and a salt repositories.

Collectively, the studies have led to valuable insights into the behaviour of spent fuel under disposal conditions. The main important findings and significant uncertainties important for future R&D are:

1. IRF values for some radionuclides may be very high (15 - 25 %) at burnups of 60 – 70 GWd/t_{HM} . This is largely due to the rim restructuring, which leads to accumulation of volatile fission products in pores in the rim. There is very little information on the leaching behaviour of higher burnup fuels and on the leachability of the rim, thus the IRF model pessimistically assumes rapid release of the fission products in pores. Similarly, the micro-structure of MOX fuel suggests that very high IRF values (~ 50 %) may be possible. Future leaching studies should focus on examining these pessimistic assumptions.
2. The uncertainties in α radiation-enhanced diffusion are large, covering several orders of magnitude. Although the contribution of this process to the IRF and to overall radionuclide release from spent fuel is not large, it would be useful to further refine the understanding to reduce the uncertainty in model predictions.
3. The effects of He buildup may be a significant issue for high burnup and MOX fuels. These aspects were not explored in the SFS Project, but should be looked at in future because build-up of high gas pressures in pores might destabilise grain boundaries, possibly leading to cracking.
4. Radiolytic models for gamma and alpha radiolysis of brine solutions have been tested and shown to have good agreement with experiments for a wide range of conditions. Nonetheless, these experiments have not dealt with production and recombination of radiolysis products at surfaces, thus more work is required in this area.

5. Experimental studies of the effects of α -radiolysis of water on UO_2 dissolution under anoxic conditions using α -doped UO_2 suggest that there is a threshold below which the effects on dissolution rate are undetectable.
6. Studies of the effect of H_2 on the dissolution of spent fuel and on α -doped UO_2 show significant reductions in the dissolution rate relative to oxidising conditions, in addition to reductions in the concentrations of molecular radiolytic oxidants in solution, suggesting that surface reactions involving H_2 may be important in suppressing surface oxidation. How this occurs is not understood in detail and should be focused on in future studies.
7. A matrix alteration model (MAM) that has a strong mechanistic basis has been developed and tested. The model uses radiolytic rate equations to calculate oxidant concentrations in solution as a function of time, for reference groundwater conditions for granite, clay and salt repositories, including an H_2 pressure of 3 bars and considering the decline of the dose rate as the fuel decays. The time-dependent concentrations are then used to calculate matrix dissolution rates as a function of time. Uncertainties in the reactive fuel surface area, radiolytic yields and evolution of solution chemistry (including corrosion products, clay and H_2 concentrations) should be further explored in order to improve this model.
8. Fractional matrix dissolution rates calculated with the MAM are in the range of $3 \times 10^{-5} \text{ yr}^{-1}$ at the presumed time of container breaching (1 000 years), gradually decreasing to $1 \times 10^{-6} \text{ yr}^{-1}$ at 10^5 years. Experimental data from various studies using spent fuel and α -doped UO_2 with H_2 overpressures suggest that the dissolution rates may be in the range of 10^{-6} yr^{-1} to 10^{-8} yr^{-1} , and it is not possible at present to comment on possible time-dependence of the rate.
9. An integrated model of spent fuel dissolution combining the IRF model and the MAM has been used to illustrate the time-dependent release of radionuclides from a container of spent fuel. The model illustrates the relative importance of various fuel-related processes involved in dissolution and retention of radionuclides.
10. Overall, the potential for spent fuel to confine radionuclides is good for low to moderate burnup fuels, in particular, work on hydrogen effects has good potential to confirm the good performance of this material as a waste form. For high burnup and MOX fuels, much work remains to be done to further examine the pessimistic assumptions of the IRF model.

9 References

- Andriambololona, Z. and L.H. Johnson. 2003. The environmental boundary conditions for the evaluation of spent fuel matrix dissolution. Unpublished Technical Note for the SFS Project, European Commission SFS Project Report, Contract No. FIKW-CT-2001-20192-SFS.
- Cachoir, C., P. Carbol, J. Cobos-Sabate, J. P. Glatz, B. Grambow, K. Lemmens, A. Martínez-Esparza, T. Mennecart, C. Ronchi, V.V. Rondinella, D. Serrano-Purroy, K. Spahiu, D.H. Wegen and T. Wiss, 2005. Effect of alpha irradiation field on long term corrosion rates of spent fuel, European Commission SFS Project Report, Contract No. FIKW-CT-2001-20192-SFS, JRC-ITU-SCA-2005/01, JRC-ITU Karlsruhe.
- Carbol, P., J. Cobos-Sabate, J-P. Glatz, B. Grambow, B. Kienzler, A. Loida, A. Martinez Esparza, V. Metz, J. Quiñones, C. Ronchi, V. Rondinella, K. Spahiu, D. H. Wegen, T. Wiss: The effect of dissolved hydrogen on the dissolution of ^{233}U doped $\text{UO}_2(\text{s})$, high burnup spent fuel and MOX fuel, European Commission SFS Project Report, Contract No. FIKW-CT-2001-20192-SFS, SKB Technical Report TR-05-09, SKB, Stockholm.
- de Pablo J., I. Casas, J. Giménez, M. Molera, M. Rovira, L. Duro and J. Bruno, 1999. The oxidative dissolution mechanism of uranium dioxide. I. The effect of temperature in hydrogen carbonate medium. *Geochim. et Cosmochim. Acta*, 63 (19/20), 3097-3103.
- de Pablo, J., I. Casas, F. Clarens, J. Giménez and M. Rovira. 2003: Contribucion experimental y modelizacion de procesos básicos para el desarrollo del modelo de alteración de la matriz del combustible irradiado. Publicacion Tecnica Enresa 01/2003.
- de Pablo J., I. Casas, J. Giménez, F. Clarens, L. Duro and J. Bruno, 2004. The oxidative dissolution mechanism of uranium dioxide. The effect of pH and oxygen. *Mat. Res. Soc. Symp. Proc.* 807, pp. 83-88.
- Ekeroth E. and M. Jonsson, 2003. Oxidation of UO_2 by radiolytic oxidants. *J. Nucl. Mater.*, 322, 242-248.
- Forsyth, R. 1997. The SKB Spent Fuel Corrosion Program, SKB Technical Report 97-25, SKB, Stockholm.
- Giménez J., Clarens F., Casas I., Rovira M., de Pablo J. and Bruno J., 2001. Oxygen consumption in uranium dioxide dissolution experiments in bicarbonate medium. Migration'01, Bregenz; to be published.
- Johnson, L. H., C. Poinssot, C. Ferry and P. Lovera. 2004: Estimates of the instant release fraction for UO_2 and MOX fuel at $t = 0$, European Commission SFS Project Report, Contract No. FIKW-CT-2001-20192-SFS, Nagra Technical Report NTB 04-08, Nagra, Wettingen, Switzerland.
- Johnson, L.H. and F. King. 2003: Canister options for the disposal of spent fuel. Nagra Technical Report NTB 02-11.
- Johnson, L.H., C. Ferry, C. Poinssot and P. Lovera. Spent fuel radionuclide source-term model for assessing spent fuel performance in geological disposal. Part I: Assessment of the Instant Release Fraction. Submitted to *J. Nucl. Mat.*

- Kelm, M. and E. Bohnert 2004: A kinetic model for the radiolysis of chloride brine, its sensitivity against model parameters and a comparison with experiments. European Commission SFS Project Report, Contract No. FIKW-CT-2001-20192-SFS. Forschungszentrum Karlsruhe Wissenschaftliche Bericht FZKA 6977, Forschungszentrum Karlsruhe GmbH, Karlsruhe..
- Lovera, P., C. Ferry, C. Poinssot & L. H. Johnson. 2003: Synthesis report on the relevant diffusion coefficients of fission products and helium in spent nuclear fuels. European Commission SFS Project Report, Contract No. FIKW-CT-2001-20192-SFS, Commissariat l'Énergie Atomique report CEA-R-6039.
- Koo, Y-H., B.-H. Lee, J-S. Cheon, & D.- S. Sohn. 2001: Pore pressure and swelling in the rim region of LWR high burnup UO₂ fuel. J. Nucl. Materials 295, pp. 213-230.
- Martínez Esparza, A., M. A. Cuñado, J. A. Gago, J. Quiñones, E. Iglesias, J. Cobos, A. González de la Huebra, E. Cera, J. Merino, J. Bruno, J. de Pablo, I. Casas, F. Clarens, and J. Giménez, Development of a Matrix Alteration Model (MAM), European Commission SFS Project Report, Contract No. FIKW-CT-2001-20192-SFS, in *Publicaciones técnicas*, vol. 1-05: ENRESA, 2005.
- Merino, J., E. Cera, J. Bruno, J. de Pablo, J. Quiñones, and A. Martínez Esparza. In press: Radiolytic modelling of spent fuel oxidative dissolution mechanism. Calibration with UO₂ dynamic leaching experiments, J. Nucl. Mat.
- Nagra 2002a: Project Opalinus Clay, Models, Codes and Data for Safety Assessment, Nagra Technical Report NTB 02-06, Nagra, Wetztingen, Switzerland.
- Nagra 2002b: The long-term safety of a repository for spent fuel, vitrified high-level waste and long-lived intermediate-level waste sited in the Opalinus Clay of the Zürcher Weinland . Nagra Technical Report NTB 02-05. Nagra, Wetztingen, Switzerland.
- Olander, D. 2004: Thermal spike theory of athermal diffusion of fission products due to alpha decay of actinides in spent fuel (UO₂). SKB Technical Report TR 04-17, SKB, Stockholm..
- SKB 1999: SR-97. Data and data uncertainties, compilation of data and data uncertainties for radionuclide transport calculations. SKB Technical Report TR 99-09, SKB, Stockholm.

Appendix 1: Mass transport conditions at the interface between the near field and the host rock

P.A. Smith (SAM Ltd.) and L.H. Johnson

For radionuclides whose concentration in the reservoir (breached container) is not constrained by solubility limits, provided the reservoir volume is small, the boundary conditions between the near field and the host rock are irrelevant to the release rate to the host rock. The release rate is determined purely by the behaviour of the fuel subsequent to container breaching. All radionuclides released from the fuel are conveyed effectively instantaneously into the host rock. This is because, apart from the fuel itself and the small reservoir, the near field has no capacity to store radionuclides.

The situation is different for radionuclides constrained by the solubility limits of the corresponding elements. For these radionuclides, once the solubility limit has been reached, radionuclides are transported into the host rock by advection, at a rate (per unit length of waste form):

$$F_{adv} = C_s Q_{GW}$$

and by diffusion at a rate:

$$F_{diff} = 2\pi a D_{HR} \left. \frac{dC}{dr} \right|_{r=a}$$

where C_s is the solubility limit, Q_{GW} is the flowrate of groundwater (per unit length of waste form) with which radionuclides become mixed, D_{HR} is the effective diffusion coefficient of the host rock, and a is the near field tunnel radius (assuming in-tunnel emplacement). dC/dr is the concentration gradient in the host rock. In the absence of a geosphere transport model, this can be approximated as:

$$\frac{dC}{dr} \approx \frac{C_s}{L_{HR}}$$

where L_{HR} is a length scale characterising the diffusive transport distance across the host rock (e.g. the thickness of the host formation).

Thus, combining all of the above:

$$F_{adv} + F_{diff} = C_s \left[Q_{GW} + \frac{2\pi a D_{HR}}{L_{HR}} \right].$$

The SPENT model assumes that advection dominates over diffusion in the host rock, so that the release from the near field to the host rock is:

$$F \approx F_{adv} = C_s Q_{GW}.$$

The user only needs to specify Q_{GW} as a host-rock dependent parameter. If, however, diffusion is also important, then an effective flowrate can be defined:

$$Q_{eff} = \left[Q_{GW} + \frac{2\pi a D_{HR}}{L_{HR}} \right]$$

and input in place of Q_{GW} so that the release calculated by SPENT is:

$$F = F_{adv} + F_{diff} = C_s Q_{eff} = C_s \left[Q_{GW} + \frac{2\pi a D_{HR}}{L_{HR}} \right]$$

as required.

D_{HR} and L_{HR} should be simple to specify for a given rock type. It will also be simple to specify a Darcy velocity, q_{HR} . In order to obtain Q_{GW} from the Darcy velocity, however, it is necessary to have some conceptual model of how radionuclides mix with the groundwater that flows around the repository near field. Suppose radionuclides released from the near field are mixed in the excavation-disturbed zone (EDZ) surrounding the repository tunnels. In this case:

$$Q_{GW} = 2q_{EDZ}(r_{EDZ} - a).$$

where q_{EDZ} [m/a] is the Darcy flux through the repository tunnel EDZ averaged along a line drawn perpendicular to the flow direction through the axis of the borehole, and r_{EDZ} is the distance from the centre of the tunnel to which the EDZ extends.

The value of q_{EDZ} depends on the geometry of the EDZ and its hydraulic conductivity with respect to the undisturbed geosphere (K_{EDZ}/K):

$$\frac{q_{EDZ}}{q_{HR}} = \frac{2 \frac{K_{EDZ}}{K} r_{EDZ} \left(\frac{r_{EDZ} + a}{r_{EDZ}^2 + a^2} \right)}{1 + \frac{K_{EDZ}}{K} \left(\frac{r_{EDZ}^2 - a^2}{r_{EDZ}^2 + a^2} \right)}$$

If $K_{EDZ}/K \gg 1$,

$$q_{EDZ} \approx 2q_{HR} \frac{r_{EDZ}}{r_{EDZ} - a}.$$

Thus:

$$Q_{GW} = 4qr_{EDZ},$$

It is proposed that we assume that the near field tunnels are surrounded by an excavation disturbed zone extending one tunnel diameter onto the host rock (i.e. out to a distance $3a$ from the centre of the tunnels / boreholes). Thus:

$$Q_{GW} = 12q_{HR}a$$

and the effective flowrate to be input in SPENT to provide a boundary condition at the near field / host rock interface is:

$$Q_{eff} = 2a \left[6q_{HR} + \frac{\pi D_{HR}}{L_{HR}} \right].$$